

Mineralogy and Microscopy of Some Sedimentary Rocks in Sarawak

by

Dexter Brian anak Nyambang

Petroleum Engineering

10643

Dissertation submitted in partial fulfilment of
the requirement for the
Bachelor of Engineering (Hons.)
(Petroleum Engineering)

JANUARY 2012

Universiti Teknologi PETRONAS

Bandar Seri Iskandar

31750 Tronoh

Perak Darul Ridzuan

CERTIFICATION OF APPROVAL

**Mineralogy and Microscopy of Some Sedimentary Rocks in
Sarawak**

by

Dexter Brian anak Nyambang

A project dissertation submitted to the
Geosciences and Petroleum Engineering Department

Universiti Teknologi PETRONAS

in partial fulfilment of the requirement for the

Bachelor of Engineering (Hons.)

(Petroleum Engineering)

Approved by,

(A.P Dr. Eswaran Padmanabhan)

UNIVERSITI TEKNOLOGI PETRONAS

TRONOH, PERAK

JANUARY 2012

CERTIFICATION OF ORIGINALITY

This is to certify that I am responsible for the work submitted in this project, that the original work is my own except as specified in the references and acknowledgements, and that the original work contained herein have not been undertaken or done by unspecified sources or persons.

(DEXTER BRIAN ANAK NYAMBANG)

ABSTRACT

Sedimentary rocks are composed principally of detrital mineral grains. The physical properties of the mineral grains which compose the sedimentary rock determine grain matrix framework compaction resistance as well as the texture of the rock itself. The study on mineralogy (crystal structure, chemistry, physical properties of mineral, descriptive mineral) and microscopic (grain size, textural maturity, shape, isotope geochemistry) properties of selected reservoir quality will be conducted on the sedimentary rocks belonging to Nyalau Formation, Sarawak. The lithofacies structure, bed geometry and etc will also be studied for the purpose of correlation and mapping. Nyalau Formation was chosen because of its' proximity location to Baram Formation (known for its oil and gas exploration and production). Currently, there are very limited informations related to mineralogy and microscopic properties in some sedimentary rocks in Sarawak. There is a lack of information in specific petrophysical properties such as Thermal Conductivity and poro-perm. There is also lack of information in relationship between fabric characteristic and their critical reservoir properties in these rocks. The possible relationship between the fabric variability and behaviour of some critical petrophysical properties in the sedimentary rocks need to be evaluated. Methodology, which is sample collection and laboratory examination, will be carried out. Samples will also be taken back to the laboratory for analysis. The mineralogy examinations will be performed by using X-ray Diffractometer (XRD), Scanning Electron Microscope (SEM), Fourier Transform Infrared Radiation (FTIR), Ultra Violet (UV), EGME Testing, Total Organic Compound (TOC), and Thin Section. Mercury porosimeter will be used to relate the pore size distribution and permeability to the mineralogical data while Thermal Conductivity will be used to estimate and understand the heat transfer or temperature between rock facies, as the feature is important in enhancing basin modelling and reservoir characteristic.

ACKNOWLEDGEMENTS

First and foremost, praise be to the Almighty God for giving an utmost opportunity for the author to accomplish this final year project as part of the requirements for Bachelors of Engineering (Hons.) in Petroleum Engineering at Universiti Teknologi PETRONAS.

Secondly the author is grateful for all the supports shown by parents. They have continuously provided moral and financial supports until the end of this project. Also a big 'thank you' to the assigned supervisor for this project, A.P Dr Eswaran Padmanabhan who has sacrificed her time in giving guidance and necessary improvements from time to time.

Not forgetting fellow postgraduate students at University Teknologi Petronas, Yasir Ali, Shama, Nurul Aiman, and Syamim Ramli for all their precious help in providing the required data and information which are sufficient for the accomplishment of this final year project.

Last but not least, the author would like to express his gratitude to fellow colleagues who have always provided moral supports and a never-ending assistance in ensuring this final year project is finished within the given time frame.

Dexter Brian anak Nyambang,

Petroleum Engineering

Universiti Teknologi PETRONAS.

TABLE OF CONTENTS

List of Figures.....	9
List of Tables.....	11
List of Abbreviation.....	11
 CHAPTER 1: INTRODUCTION.....	 13
1.1 Project Background.....	14
1.2 Problem Statement.....	13
1.3 Objectives.....	14
1.4 Scope of Study.....	14
1.5 Relevancy of Project.....	14
1.6 Feasibility of Project.....	15
 CHAPTER 2: LITERATURE REVIEW.....	 16
2.1 Literature Review.....	16
2.1.1 Introduction.....	16
2.1.2 Reservoir and Petrophysical properties of Sedimentary Rock.....	16
2.1.3 Stratigraphic of North and Central Sarawak.....	17
2.2 Nyalau Formation.....	20
2.2.1 Facies Description.....	21
2.2.2 Mineralogy.....	22
2.2.3 Orientation of Particles.....	24
2.2.4 Grain Size and Distribution.....	24
2.2.5 Porosity-Permeability.....	25

2.2.6 Density.....	25
2.2.7 Thermal Conductivity.....	25
CHAPTER 3: MATERIALS AND METHODS.....	35
3.1 Flow Work.....	35
3.2 Study Area.....	35
3.2.1 Outcrop 1.....	36
3.2.2 Outcrop 2.....	36
3.2.3 Outcrop 3.....	37
3.3 Research Methodology.....	37
3.3.1 Mineralogy.....	38
3.3.2 Microscopic.....	39
3.3.3 Chemical Composition.....	41
3.3.4 Petrophysical.....	45
3.4 Project Activities.....	47
3.5 Key Milestone.....	47
CHAPTER 4: RESULTS AND DISCUSSIONS.....	48
4.1 Thermal Conductivity.....	48
4.2 Fourier Transform Infrared Radiation.....	49
4.3 Ultraviolet.....	54
4.4 X-ray Diffraction.....	55
4.5 Ethylene Glycol Monoethyl Ether.....	57
4.6 Total Organic Carbon.....	58
4.7 Hg Porosimeter.....	59

4.7.1 Pore Size Distribution.....	60
4.8 Scanning Electron Microscope.....	63
4.9 Thin Section.....	65
4.10 Evaluation of Fabric Variability onto Petrophysical Properties.....	67
4.10.1 Fabric variability and petrophysical properties onto Thin Section.....	67
4.10.2 Thermal Conductivity vs Total Organic Carbon.....	68
4.10.3 Thermal Conductivity vs Porosity.....	69
 CHAPTER 5: CONCLUSIONS AND RECOMMENDATIONS.....	71
5.1 Conclusion.....	71
5.2 Recommendation.....	72
 REFERENCES.....	74
 APPENDICES.....	76

LIST OF FIGURES

Figure 1	Map of Borneo Island. Nyalau Formation situated at Bintulu, Sarawak.....	18
Figure 2	Lithostratigraphic summary from east of Bintulu to west of Miri (Haile and Ho, 1991). Suggested stops 1 to 7 are indicated. Right: simplified road map northwards from southern base of Lambir Hills.....	19
Figure 3	Stratigraphy of the Bintulu - Tatau area (Wolfenden, 1960; Bait and Asut, 1991).....	21
Figure 4	Comparison between logged sections at (a) Sungai Selad, Bintulu - Tatau Road and (b) Km 16, Bintulu - Miri Road (Area within Nyalau Formation).....	23
Figure 5	Histogram of bioturbated mudstone and hummocky cross-stratified sandstone interbedding, facies of Nyalau Formation.....	24
Figure 6	Thermal Conductivity of sedimentary rocks, subdivided according to chemical or physical sedimentation processes.....	27
Figure 7	Sedimentary rock. Two curves are shown for carbonates (limestone and dolomite) and clastic sediments, i.e. (quartz) sandstone and shale.....	27
Figure 8	Fig A (Thermal conductivity for different rock samples based on frequency).....	30
Figure 9	Fig B (the thermal conductivity for the different facies and lithologies vary.....	30
Figure 10	Graph showing the relationship between thermal conductivity and rock porosity.....	33
Figure 11	Graph showing the relationship between thermal conductivity and the particle size.....	34
Figure 12	Work flow for FYP I & FYP II.....	35

Figure 13	Location of the study area in Nyalau Formation.....	35
Figure 14	Unit 1 & Unit 3 of Outcrop 1.....	36
Figure 15	Unit 1 Outcrop 2.....	36
Figure 16	Unit 3 and Unit 7 of Outcrop 3.....	37
Figure 17	Laboratory experiment according to 4 categories (mineralogy, microscopy, chemical and petrophysical).....	37

Pore Size Distribution of Hg Porosimeter (Figure 18 – Figure 22)

Figure 18	U1 OC1.....	60
Figure 19	U3 OC1.....	60
Figure 20	U1 OC2.....	61
Figure 21	U3 OC3.....	61
Figure 22	U7 OC3.....	62

Scanning Electron Microscope (Figure 23 – Figure 27)

Figure 23	U1 OC1.....	63
Figure 24	U3 OC1.....	63
Figure 25	U1 OC2.....	63
Figure 26	U3 OC3.....	63
Figure 27	U7 OC3.....	63

Thin Section (Figure 28 – Figure 32)

Figure 28	U1 OC1.....	65
Figure 29	U3 OC1.....	65
Figure 30	U1 OC2.....	65
Figure 31	U3 OC3.....	65
Figure 32	U7 OC3.....	65

Figure 33	Thermal Conductivity vs. T.O.C.....	68
Figure 34	Thermal Conductivity vs. Porosity.....	69

LIST OF TABLES

Table 1	Thermal conductivity values for some of the sandstone and shale from Belait Formation.....	32
Table 2	Weathered Surfaces.....	48
Table 3	Inner Surfaces.....	48
Table 4	Overall Thermal Conductivity Coefficients.....	49

Fourier Transform Infrared Radiation (Table 5 – Table 9)

Table 5	U1 OC1.....	49
Table 6	U3 OC1.....	50
Table 7	U1 OC2.....	51
Table 8	U3 OC3.....	52
Table 9	U7 OC3.....	53
Table 10	E4/E5 Ratio.....	54
Table 11	XRD Results.....	55
Table 12	EGME Results.....	57
Table 13	TOC Results.....	58
Table 14	Hg Porosimeter Results.....	59

LIST OF ABBREVIATIONS

<i>k</i>	Thermal Conductivity value
<i>SSA</i>	Specific Surface Area
<i>mD</i>	MilliDarcy
FTIR	Fourier Transform Infrared Radiation
EGME	Ethylene Glycol Monomethyl Ether
TOC	Total Organic Carbon
Hg	Mercury
SEM	Scanning Electron Microscope
XRD	X-Ray Diffraction
UV-VIS	Ultra Violet Visible Spectroscopy
U1 OC1	Unit 1 Outcrop 1
U3 OC1	Unit 3 Outcrop 1
U1 OC2	Unit 1 Outcrop 2
U3 OC3	Unit 3 Outcrop 3
U7 OC3	Unit 7 Outcrop 3

CHAPTER 1: INTRODUCTION

1.1 PROJECT BACKGROUND

Most of the well drilled in Malaysia are found at offshore, both West and East Malaysia. But there is less significant of research in terms of reservoir behaviour at onshore, especially in Sarawak. Most studies had been conducted around Sarawak (Miri Formation, Nyalau Formation, Crocker Formation, Belaga Formation, Kuching Formation etc; Teoh; 2007 & Hutchison; 1997). This study is important in Sarawak because it helps in determine the possibility of oil and gas exploration and production in Sarawak. This project will focus on Nyalau Formation, which involve the analysis and study of mineralogy and microscopic found in some sedimentary rocks there. By studying these two segments, it is known that fabrics of sedimentary rocks control the petrophysical properties such as porosity, permeability, density and others. According to initial research, majority of the formations in Sarawak (Nyalau, Belaga etc) indicated low to medium poro-perm, which means very low reservoir qualities. The study of mineralogy and microscopic onto several collected samples helps to determine the patterns and behaviours of selected outcrops in Nyalau Formation whether the outcrops are a potential reservoirs or not.

1.2 PROBLEM STATEMENT

The study on mineralogy and microscopical properties onto selected reservoir sedimentary rocks in Sarawak is still lacking in information. There is also a lack of information of specific petrophysical properties such as thermal conductivity, where much of the thermal conductivity data reported in the previous literature are lacks a complete description of the physical properties of the rock used, and in addition, most of the thermal conductivity measurement have been made at room temperature and at atmospheric pressure. The relationship between critical reservoir properties and the fabric characteristic in these rocks also needs to be studied.

1.3 OBJECTIVE

The main objective is to investigate the relationship between fabric variability and behaviour of selected critical petrophysical properties in some sedimentary rocks found in Sarawak.

1.4 SCOPE OF STUDY

The scope of study of this research revolves around the characteristic of mineralogy and microscopic properties found in the sample. By doing the identification and classification of each elements found in the samples, the types and characteristics of sedimentary rock can be determined. Parameters obtain from the sedimentology facies and mineral(s) properties will also help to establish the link between fabric variability and some critical petrophysical properties found with the selected potential reservoir sample.

Lithofacies will also be among the scope of study. Lithofacies are obtained based on the lithology of the outcrops, sedimentary structures, rocks composition and bed geometry. Lithofacies can also be used for the purpose of mapping and correlation of the field of study.

1.5 RELEVANCY OF PROJECT

The relevancy of this project poses a great deal of significant onto geological study, especially in the interior parts of Sarawak. For this project, the author will apply his theoretical and practical knowledge from Petroleum Engineering into geological field. The study is also relevance as the study field involves Nyalau Formation. Recently, there was a signing on ‘Head of Agreement’ between Petronas and Shell for two, 30 years PCSs for developing and enhancing the EOR project on Baram Delta (www.shell.com.my; 2011). Since Baram Delta is known for its vast reservoir field that has gone through oil and gas exploration and production, Nyalau Formation

is just located to the south-east of the Baram Formation. Nyalau Formation is considered an 'area of interest' because of its nearby location.

1.6 FEASIBILITY OF PROJECT

All objectives stated earlier are achievable and feasible in terms of this project duration and timeframe. The site visit and samples collection had been done early December 2011, where the field trip was done in Tatau, Bintulu-Sibu road. Three outcrops had been chosen within Nyalau Formation. The author also has knowledge on geology courses such as Petroleum Geosciences, Reservoir Rock and Fluid Properties, as well as journal and research papers related to Geology, Geosciences, Geochemistry and Geophysicists. All these materials are available in the university library and related website. The experiments will be done back in university laboratories where all the necessary equipments are available at laboratory.

CHAPTER 2: LITERATURE REVIEW

2.1 LITERATURE REVIEW

2.1.1 Introduction

The main aim of this study is to describe, characterize and quantify the selected reservoir quality sedimentary rocks based on the mineralogy and microscopy found within the samples by integrating both mineralogy and microscopic properties. Sedimentary rocks are the result of sedimentation processes, originating from older igneous, metamorphic and previously deposited sediments that have been broken down physically and chemically. Sedimentation process is the process of deposition of particles carried by a fluid flow. This results in the formation of depositional landforms and the rocks that constitute sedimentary records. The weathered material is transported as debris and accumulated at the locus of deposition. (Teoh et al., 2007)

2.1.2 Reservoir Rocks and Fluid Properties

Sedimentary rocks are common reservoirs rocks for oil and gas. Knowledge of their properties is essential in the exploration for, and the production of subsurface fluids. It is essential to understand the reservoir capacity for oil and gas production. Most reservoir studies require that geologic variables be handled in a quantitative manner. For the purpose of analysis, it is important to categorize reservoir rock properties so that interrelationships among the variables may be recognized.

Rocks are homogeneous or inhomogeneous in a considered volume; this pair of terms indicates whether the property is a function of local coordinates within the volume or not. Rocks are also isotropic or anisotropic in a considered volume; this pair of terms indicates whether the property is a function of direction or not. The

property is equal in all directions and can be used as a scalar in the case of isotropy. The property depends on direction and must be used as tensors align with its symmetry in the case of anisotropy. (Schon et al; 1996)

Petrophysical properties of sedimentary rocks are influenced by porosity, permeability, velocity and density; these properties are partly controlled by facies characteristics which in turn are related to depositional processes. To predict the movement of hydrocarbon in a reservoir, the transportation in an underground aquifer or weathering processes and stone decay in numerous architectural structures, these petrophysical properties are very important and needed. (Teoh et al; 2007)

2.1.3 Stratigraphic of North Borneo

North of Sarawak refers to Miri and its surrounding formation while Central of Sarawak refers to Bintulu and its surrounding formation. The Late Eocene and younger stratigraphic (post-Sarawak Orogeny) of the Miri Zone (North part of Sarawak) is wholly of molasse. The strata were deposited in non-marine to inner neritic marine conditions and local unconformities are common as a result of long-ranging thin-skinned compression tectonics. The basement of the Miri Zone, at least in considerable part, is of Rajang Group flush, which has been thrust up in compression steeply dipping and complexly folded anti-formal structures to form inliers, bearing local names such as Bawang Member of the Belaga Formation, Kelalan Formation and Mulu Formation. They are all remarkably similar and of sandstone-shale laminate turbidity. (Hutchinson et al; 2005)



Figure 1: Map of Borneo Island. Nyalau Formation located at Bintulu, Sarawak

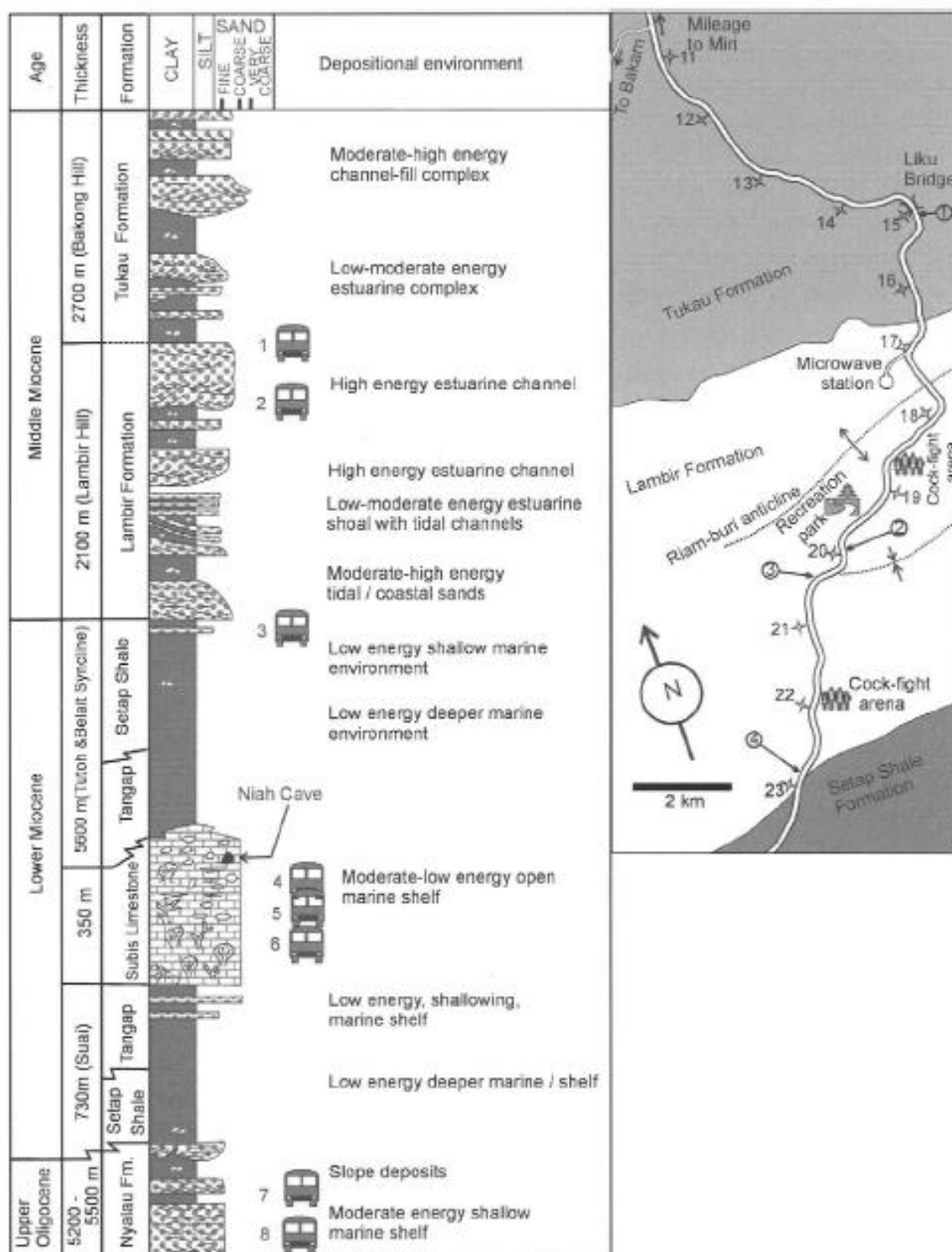


Figure 2: Lithostratigraphic summary from east of Bintulu to west of Miri (Haile and Ho, 1991). Suggested stops 1 to 7 are indicated. Right: simplified road map northwards from southern base of Lambir Hills.

2.2 Nyalau Formation

The Nyalau Formation of Bintulu area, Sarawak occurred as:

- i. Offshore - subtidal estuarine sandstones, sandy shales, and shales with dispersed lignite bands and marls.
- ii. Silty sandstone interval partly calcareous and grading into sandy-limestone
- iii. Biban sandstone Member with Oligocene-Miocene age which consists of fine to medium-grained sandstones and siltstones with calcareous nodules.
- iv. Kakus Member of this formation with Lower-Middle Miocene age which consists of massive sandstone intervals, laminated clays, and brackish-shales and lignites

(Liechti & Haile, 1960)

The Nyalau Formation was deposited during the Late Oligocene (25 Million Years) to Early Miocene (10 Million Years). Nyalau Formation consists of hard fine to medium grained sandstones alternating with shale as well as contains coal beds and infrequently thin limestone. The sandstones show cross-bedding and are rippled. The Heterolithic parasequences contain sandstone which is moderately bioturbated by Ophiomorpha (Hutchinson et al., 2005; Shushan & Hadi, 2007). Environment of deposition ranged from lower coastal plain to estuarine, shallow littoral to inner neritic. The total thickness of the formation is variously estimated to be 5000-5500 m. To the east, the Nyalau is conformably overlain by the Sibuti and to the northeast it interfingers with the shaly Setap Shale. Common stratigraphy of Nyalau Formation is inter-bedded sand-shale, which can be seen at the location. This suggests the alternating of low and high energy. The sand layer contains burrows which indicate marine environment and shale layer could be deposited in protected area. (Hutchinson et al., 1997)

Originally, Nyalau Formation is of importance as it is an onshore extension of the Balingian Province offshore Sarawak and is considered to contain important source and reservoir rocks for oil and gas (Du Bois; 1985). In offshore areas, the sediments consist of fluvial and estuarine channel sands with overbank clays and coals. Selected crude oils from the Balingian Province are waxy (high proportion of nC₂₀₊) with high pristane/phytane ratio of >3.0 suggesting the source rock to have

been deposited in peat swamp environment of deposition (Awang Sapawi et al., 1991).

2.2.1 Facies Description

System	Period	Formation	Depositional facies
Tertiary	Miocene		
		Nyalau	Shallow marine, tidal and coastal plain deposits
	Oligocene	Buan	Shallow marine, shelf deposits
		Tatau	Deep marine, 'proximal' turbidites
	Upper Eocene	Belaga	Deep marine, 'distal' turbidites

Figure 3: Stratigraphy of the Bintulu - Tatau area (Wolfenden, 1960; Bait and Asut, 1991)

The onshore Nyalau Formation is made up of a similar lithological sequence of sandstone, shale, mudstone, and also contains coal seams. These seams are generally thin, about 20-30 cm thick and rarely exceeding 1 meter (Figure 2). Examples of such onshore successions are found in the Bintulu area. The formation contain weak to moderate strong, siltstone and mudstone alternating with thin to medium thickness of sandstone. Mostly it is well-bedded, with fine to medium grained sandstone surrounding the formation. The total thickness of the Nyalau Formation is approximately 18000 ft (Liechti et al., 1960) and coals are mainly present in the middle and upper parts of the formation. The whole sequence represents shallow marine, tidal and coastal plain deposits and is only moderately folded.

2.2.2 Mineralogy

The oil-generating potential of coals and other organic rich sediments from the Late Oligocene to Early Miocene of onshore extension of Nyalau Formation is believed to be a major source rock. Coals of the Nyalau Formation are typically dominated by vitrinite. Vitrinite is a type of maceral, where "macerals" are organic components of coal analogous to the "minerals" of rocks.

Significant amount of clays minerals are also present in the coals and contain carbargilites, a clay mineral which present within coals and contain between 15% - 65% of mineral matters by volume. The sample analyzed previously, shows that the range from sub-bituminous to high volatile bituminous rank, possessing vitrinite in the range 0.42% to 0.72%. Maximum temperature values range from 4258 to 4508°C which is in good agreement with vitrinite data.

Good oil generating potential is anticipated from these coals and carbargilites with moderate to rich exinite content (15 - 35%). Petrographically, the most significant evidence of the oil-generating potential in the coals is the exsudatinitite. Exsudatinitite is a secondary mackerel, commonly to represent the very beginning of oil-generation in coal. The precursor of exsudatinitite in these coals is the maceral bituminite which readily expels to hydrocarbon-like material in the form of oil smears or exsudatinitite, as observed under the microscope.

The Bituminite (a kind of mackerel in oil-shale) is considered to play a major generative role via early exsudatinitite generation, which is considered to facilitate the overall expulsion process in coal source rocks. (Hasiah et al., 1997) There are no weatherable minerals in the sand and silt fractions, as quartz being almost exclusively present. The clay fraction is dominantly kaolinite with slight traces of mid-layer clays (Andriesse et al., 1929).

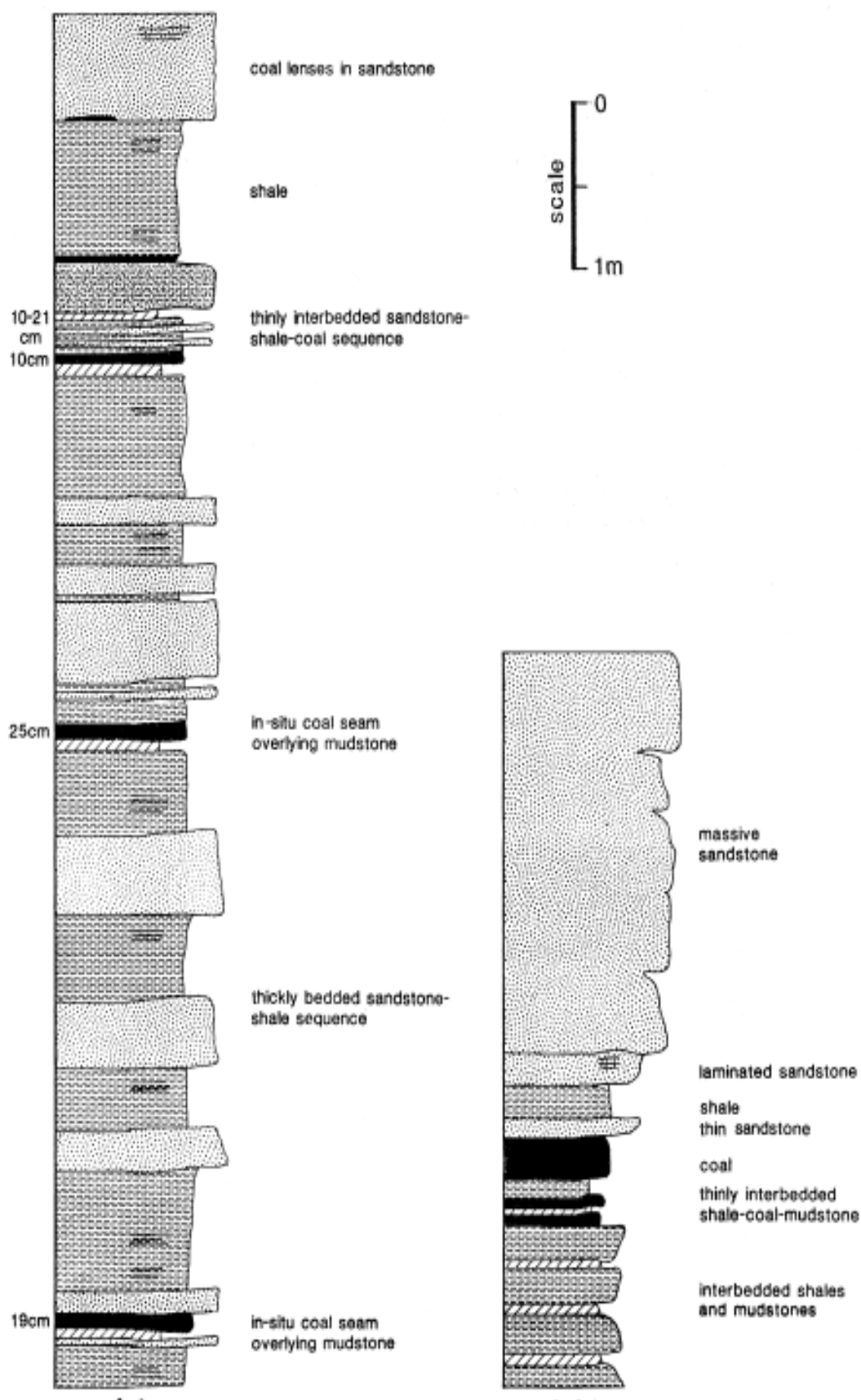


Figure 4: Comparison between logged sections at (a) Sungai Selad, Bintulu - Tatau Road and (b) Km 16, Bintulu - Miri Road (Area within Nyalau Formation)

2.2.3 Orientation of Particle

The Nyalau Formation is quite similar to the Gading Formation, except for the colour, in which Nyalau Formation is yellow to brownish yellow at depth. The soils are commonly deep with a very homogeneous profile without any apparent horization. The texture ranges from a sandy loam in the surface horizon to a sandy clay loam in the lower subsoil. The clay content increases from 15% in the surface horizon to 25% or 30% in the lower subsoil. (Andriesse et al., 1929)

2.2.4 Grain Size Distribution

The Nyalau Formation contain medium to coarse grained quartzite sandstones. Structure is weakly developed and crumbly in the surface horizon, becoming blockier with depth. Thus, the soils are friable throughout coming more firms with depth. (Andriesse et al., 1929) The phi value is more than 4.00, which is siltstone to claystone. The sorting is relatively poor with slightly bimodal according to the distribution pattern in Fig 4. The coarser mode may have been introduced by the bioturbation (Teoh & Hadi, 2007)

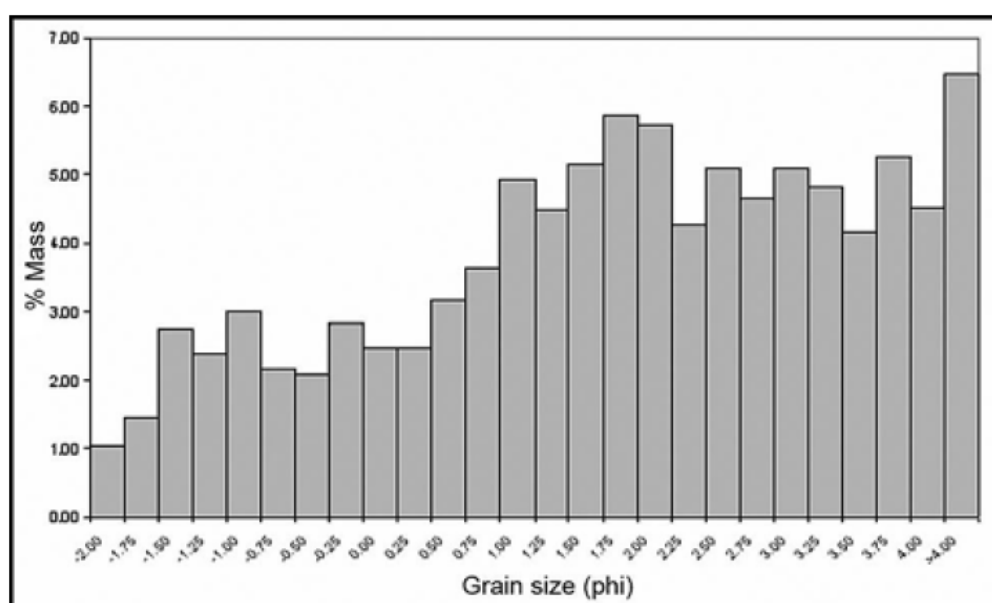


Fig 5: Histogram of bioturbated mudstone and hummocky cross-stratified sandstone interbedding, facies of Nyalau Formation

2.2.5 Porosity and Permeability

Previous sample taken from Nyalau Formation has indicated that for poro-perm values; range of 13% to 16% of porosity and 1.05mD – 8.87mD of permeability. This shows that porosity is high in surface area but diminishes with depth. The value clearly suggests that Nyalau Formation is much older and compacted compare to other formation in Sarawak (Teoh & Hadi, 2007)

2.2.6 Density

Nyalau Formation has a very high density value, which is more than 2 g/cm^3 . The average is $2.05\text{ g/cm}^3 - 2.37\text{ g/cm}^3$. (Teoh & Hadi, 2007)

2.2.7 Thermal Conductivity

Thermal Conductivity, k , is a key variable in thermal modelling because it controls the temperature within the sedimentary basins. Thermal conductivity is also used to understand heat transfer between different rock facies as well as enhance basin modelling and reservoir characteristic (Clausner & Huenges, 1995). The temperature gradient as a result of conduction is described by Fourier's law as inversely proportional to the thermal conductivity for a given heat flow:

$$Q = -k \, dT/dZ$$

Where Q is heat flow (W m^{-2}), k is thermal conductivity ($\text{W m}^{-1} \text{K}^{-1}$) and dT/dZ is temperature gradient. In 1989 Blackwell and Steele concluded that information is too sparse to estimate mean thermal conductivity effectively for a section of sedimentary rocks and, if the mean conductivity cannot be accurately predicted, even the most sophisticated modelling technology are not sufficient for accurate temperature predictions. There are still lacks of basis knowledge about thermal conductivity of sedimentary rocks and reliable information for mudstones and shale is scarce (Kristi & Elen, 1999). The statement above have proves that

thermal conductivity of sedimentary rocks in Sarawak is very lack in information, as stated in the Problem Statement.

Thermal Conductivity results may vary by as much as a factor or two for any sedimentary rocks. This is due to the natural variation of a rock's mineral content and petrophysical properties. All rocks are arranged into four basic groups characterizing the special conditions regarding their formation, metamorphism, and deposition: sediment, volcanic, plutonic, and metamorphic. For this literature review, since there is very limited information of thermal conductivity related to Sarawak's onshore formation, available and classified thermal conductivity data are acquired from several rock name and origin in several compilations. Each of the group will be studied on its statistical quantities (histogram, mean, median and standard deviation) and investigate the variation of thermal conductivity with those factors that have most effect on this group of rock. For this case, we will be studying sedimentary rock. Here is an example of thermal conductivity related to sedimentary rocks;

For Fig 6, the histogram shows that, for sedimentary rock, the controlling factors on thermal conductivity are porosity and origin of particular sediment. It seems as chemical sediments, formed by precipitation of dissolve minerals or by compaction organic material and low porosity (less than 35%) physical sediments, formed by the compaction and cementation of clastic material, have nearly identical frequency distributions, means, and median. Low porosity indicates high thermal conductivity value. The opposite side, which is in high porosity (more than 80%) probably because of marine deposited sediment, shows low thermal conductivity value. (Clausner & Huenges, 1995)

For Fig 7, effect of temperature onto sedimentary rocks shows that, up to 300°C, there is a reduction by nearly a factor of two, both for clastic and carbonaceous sediment. Above 300°C, the decrease in thermal conductivity slowly comes to an end, with carbonates decreasing still a little more than clastic sediments. However, the data for the temperature reading may vary between the past experiments with the future experiment's results, as the last observation so not have a clear view. (Clausner & Huenges, 1995)

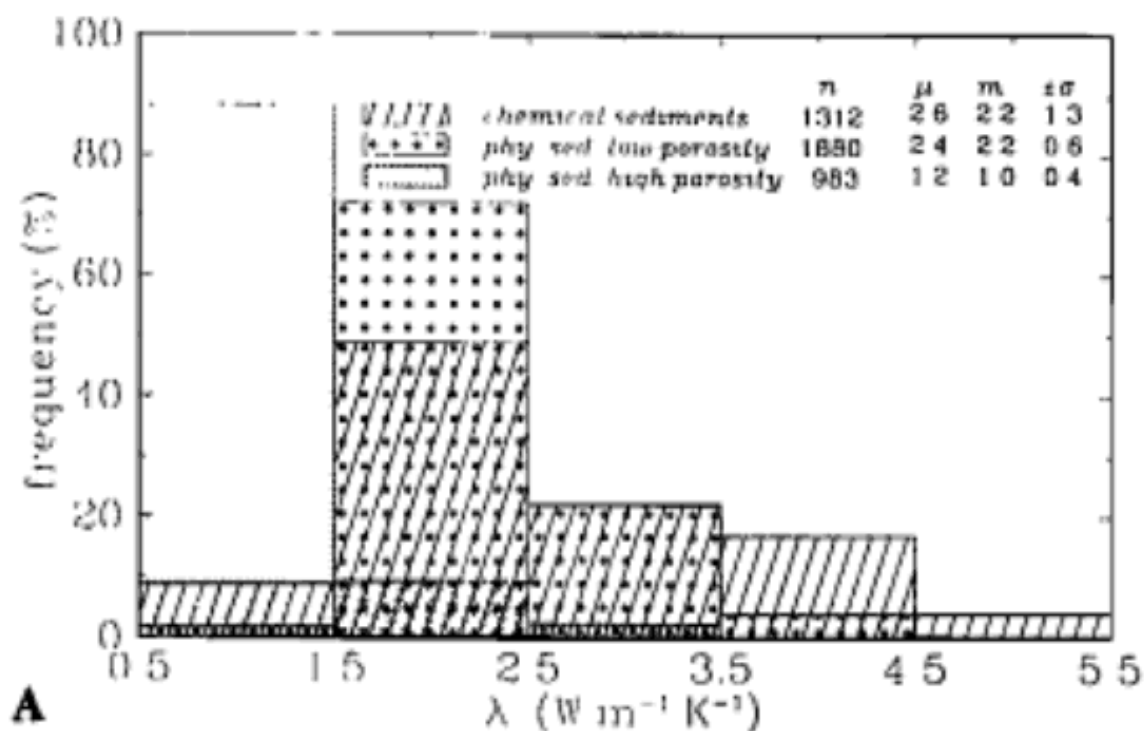


Fig 6: Thermal Conductivity of sedimentary rocks, subdivided according to chemical or physical sedimentation processes

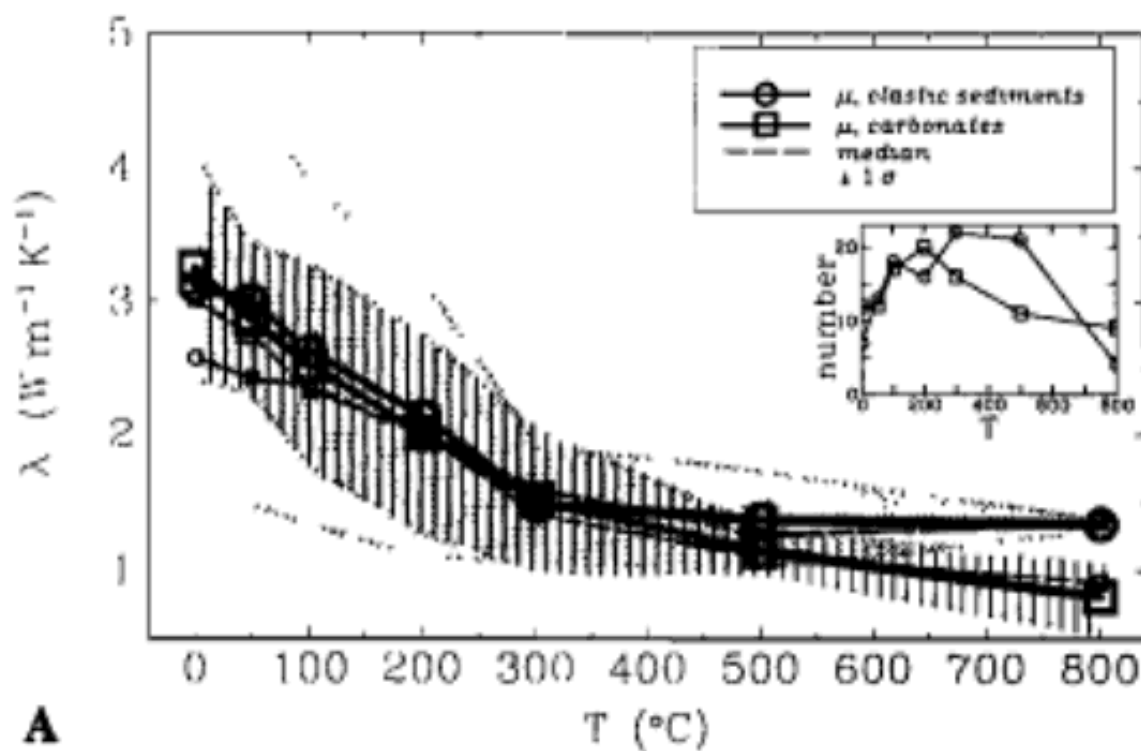


Fig 7: Sedimentary rock. Two curves are shown for carbonates (limestone and dolomite) and clastic sediments, i.e. (quartz) sandstone and shale

Thermal conductivity of different rock facies is very important especially in oil and gas exploration. Knowledge of the thermal conductivity would provide the basis of proper understanding of the behaviour of rocks and its facies at a certain depth at which the source rock would mature as well as predicting the properties of hydrocarbon (either oil or gas). The thermal conductivity of rocks also provides other relevant data such as indication of pressure, temperature and volume of the fluid in the subsurface.

Thermal conductivity in sedimentary rocks is influence by several paramount factors such as;

- Chemical composition
- Fluid content
- Fabric of the sample sedimentary rock

High porosity causes lower thermal conductivity because of air and other fluids like water infill the pores of the rock compared to the mineral. Unfortunately, thermal conductivity reading is not so accurate based on several past reports (Padmanabhan et al., 2010)

Apart from temperature, thermal conductivity also varies with pressure, degree of saturation, pore fluid, dominant mineral phase and anisotropy;

Pressure: The effect of overburden pressure is twofold, different for two distinct pressure ranges. First, fractures and micro cracks developed during stress release, when the sample was brought to the surface, begin to close again with increasing pressure. This reduces thermal contact resistance as well as porosity, which is usually filled with low conductivity fluid. If pressure is still further increases the second effect becomes apparent, the reduction of the rock's intrinsic porosity, i.e. that which is not artificially created by stress release.

Porosity and Saturating Fluid: If porosity is important, the saturating fluid's thermal conductivity may significantly affect the bulk thermal conductivity of the saturated rock. Results from three low conductivity saturate, water, oil, and air with room-temperature conductivities of about 0.6, 0.12-0.17 and 0.025 W m⁻¹K⁻¹, respectively (Grigull & Sandner, 1990). The resulting bulk conductivity behaves

according to the saturant's thermal conductivity. Additionally, contact resistances during measurements on dry rock will also reduce thermal conductivity.

Partial saturation: The effect of partial saturation varies depends whether the rock is porous or fractural. Porosity in porous rock consists of “bottlenecks” formed at the contact between individual grains and the bulk pore space. Dry bottleneck acts as thermal contact resistance between grains, while the bulk pore volume contributes according to the size to the effective thermal conductivity. If only fractures contribute to the total porosity, such as in crystalline rock, the pore space consists of bottlenecks only, and we only observe this effect alone. Porous rocks with a considerable amount of bulk pore volume will display a linear conductivity increase within the first 10% of saturation.

Dominant mineral phase and anisotropy: Figure A demonstrates the dependence for two particular metamorphic rock types, low-conductivity amphibolites, and high conductivity gneiss. Apart from the shift between the two histograms which is due to the different mineral content, the figure A also illustrate the effect of anisotropy: measurement on both rock types were performed parallel and perpendicular to the apparent direction of foliation. Amphibolite's means, median and histogram are nearly identical for either direction, as this is not the case for gneiss. The means and medians differ by about 20% and the histograms are skewed towards lower values for measurements perpendicular and towards higher values for measurements parallel to foliation. By referring to Figure B (directional dependence between the two rock samples), it is quite apparent that thermal conductivity for same rock may vary from 100% (parallel) to about 60% (perpendicular), depending on the azimuth of the measurement relative to the foliation. The variation of thermal conductivity in the amphibolite sample is less than about 5%. It is interesting to note that the amount of anisotropy is identical irrespective of the state of saturation of the sample. Comparing to seismic velocity, this indicate that anisotropy of thermal conductivity does not seem to be influences by the pore-space of fracture geometry and the saturation of this rock. This is valid as long as the fluid's thermal conductivity is less than the rock's (Clauser & Huenges, 1995)

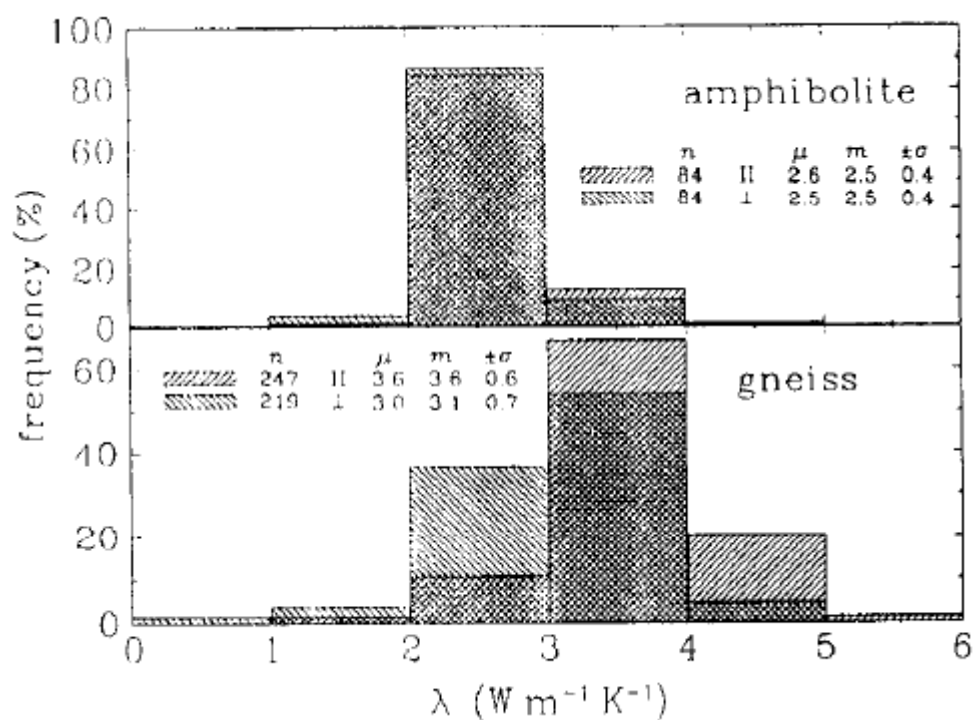


Figure 8: Fig A (Thermal conductivity for different rock samples based on frequency)

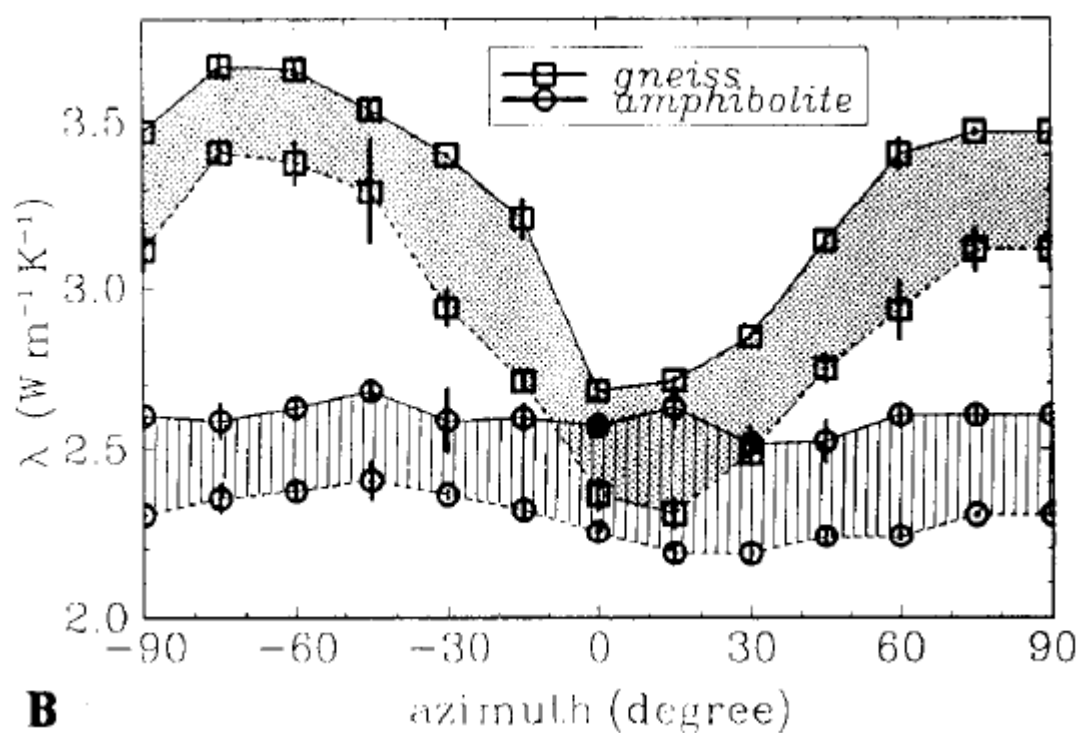


Figure 9: Fig B (the thermal conductivity for the different facies and lithologies vary)

Thermal conductivity can be measured in laboratory onto the rock samples, i.e. cores or cutting, or in-situ in boreholes or with marine heat flow probes. The most prominent being the 'divided bar' and the 'needle probe' method. This method has been discussed in several textbook and review articles (Beck; 1965, 1988, Davis; 1988, Desai et al; 1974, Somerton; 1992) and considered to be widely accepted. (Clauser & Huenges, 1995)

Nyalau Formation does not have any thermal conductivity database. For reference and example, we use Belait Formation, as it has its own thermal conductivity data. Since Belait Formation located to the north of Nyalau Formation, we consider Nyalau Formation as an 'area of interest'

The result shows that the thermal conductivity for the different facies and lithologies vary (Fig 9). Generally, sandstones should have much higher thermal conductivity values compare to shale. The reason lied in the mineralogy. Quartz in sandstones has higher conductivity compare to clay minerals. Thermal conductivity values are around 6.6 - 13 for quartz with mean values of 2.9 for clay minerals. The thermal conductivity of pure sandstone or laminated sandstone - shale, sandstone with mud drapes and with mud clasts have different values (Fig 9) Porosity and particle size of samples can also influence the thermal conductivity (Pabmanabhan et al., 2010)

Sample No.	Temp Different (T1- T2)	Length (m)	Area (m ²)	Thermal Conductivity (W m ⁻¹ k ⁻¹)	Particle Size (mm)	Estimated Porosity (%)
1	-43.2	0.011	0.0006	1.762752715	0.3500	25
2	-0.9	0.027	0.0012	207.6843198	0.0020	1
3	-41.8	0.039	0.0025	6.459081717	0.2500	15
5	-38.3	0.031	0.0023	5.603319334	0.0020	2
6	-11.6	0.022	0.0031	13.1294685	0.4000	20
9	-44.9	0.024	0.0014	3.700388772	0.0030	3
10	-11.6	0.014	0.0017	8.355116315	0.0035	4
13	-4.2	0.013	0.0020	21.42774728	0.0030	2
21	-26.5	0.005	0.0005	1.306190691	0.2000	25
23	-30.5	0.026	0.0014	5.901412367	0.0060	22
24	-27.5	0.018	0.0014	4.531294251	0.0030	2
26	-15.5	0.014	0.0005	6.252861242	0.0030	2
27	-21.9	0.02	0.0018	6.322201517	0.1700	23
35	-24.4	0.016	0.0019	34.76870122	0.0950	18
37	-9	0.01	0.0008	7.692011846	0.0800	20
39	-20	0.016	0.0010	78.81773399	0.4000	30
43	-8.2	0.033	0.0036	27.86009169	0.0700	15
44	-41.9	0.021	0.0016	3.469666441	0.0030	1.5
45	-21.2	0.031	0.0023	10.12297785	0.0035	2.5
46	-46.3	0.023	0.0017	3.438977218	0.0030	2
47	-16.8	0.018	0.0012	90.95318943	0.3000	20
49	-29.4	0.02	0.0010	69.41552131	0.0630	10
53	-9.4	0.005	0.0009	61.77873329	0.0030	2
55	-8.8	0.013	0.0010	152.6108189	0.0037	2
59	-22.2	0.014	0.0008	77.47305045	0.0850	15
63	-21.6	0.013	0.0026	23.14814815	0.0700	10
66	-32.8	0.041	0.0039	8.653513326	0.0630	10
72	-22.8	0.017	0.0022	5.161744791	0.004	8
79	-16.7	0.009	0.0017	32.07869974	0.063	5
82	-18.9	0.022	0.0011	110.8591585	0.2300	18

Table 1: Thermal conductivity values for some of the sandstone and shales from Belait Formation

Thermal Conductivity vs. Porosity

The result suggests that smaller particle sizes and lower porosities give high thermal conductivity value (Fig 10). Thermal conductivity drops steeply with increasing porosity up until porosity value of around 10%. Subsequently, the thermal conductivity appears to be fairly constant with increasing porosity. These results also provide an indication on type of overburden pressure experience by their rocks. Difference in thermal conductivity among other groups of rocks (sandstones, siltstone, or shale) can also be explained by a possible reduction in porosity due to increase in overburden pressure, thus result an increase in thermal conductivity. (Padmanabhan et al., 2010)

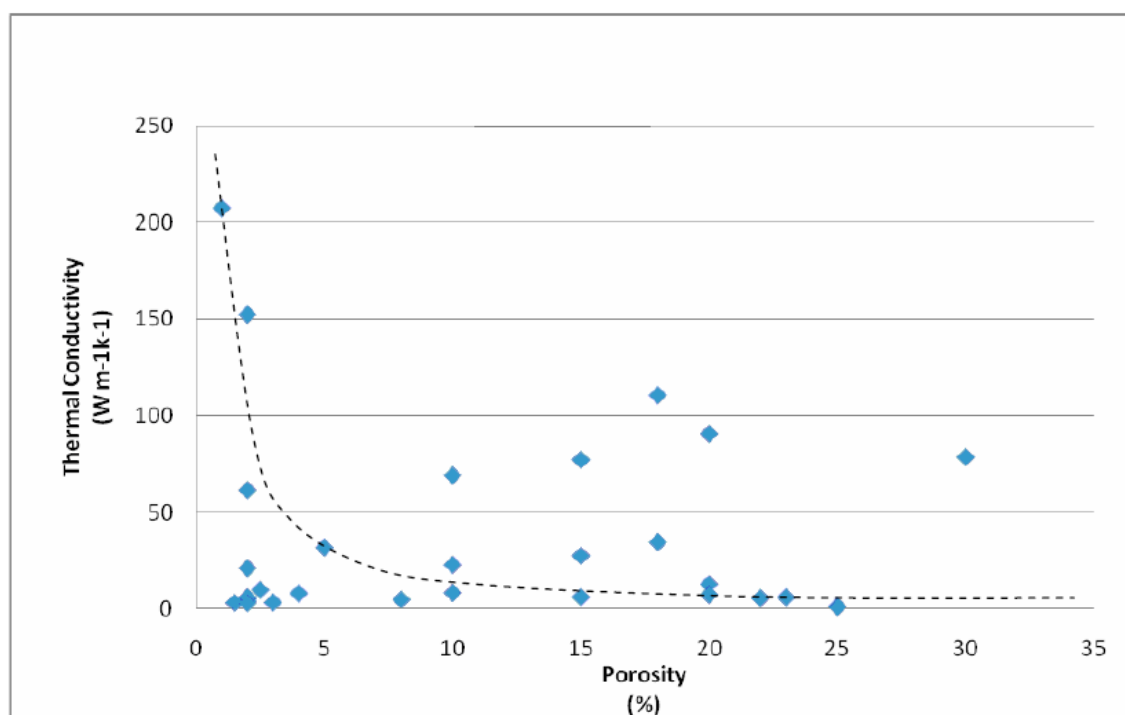


Fig 10: Graph showing the relationship between thermal conductivity and rock porosity

Thermal Conductivity vs. Particle Size

The thermal conductivity drops steeply between clay to silt size (0 – 0.05mm) (Fig 11). This suggests that argillaceous materials have high thermal conductivity. Subsequent to the initial steep decrease, thermal conductivity decrease at a much slower rate until particle size approaches very fine sand (0.15mm). Thermal conductivity remains constant when the particle size is larger than very fine grain size (> 0.15mm). The data clearly shows that sand, clay and silt tend to have different ranges of thermal conductivity. (Padmanabhan et al., 2010)

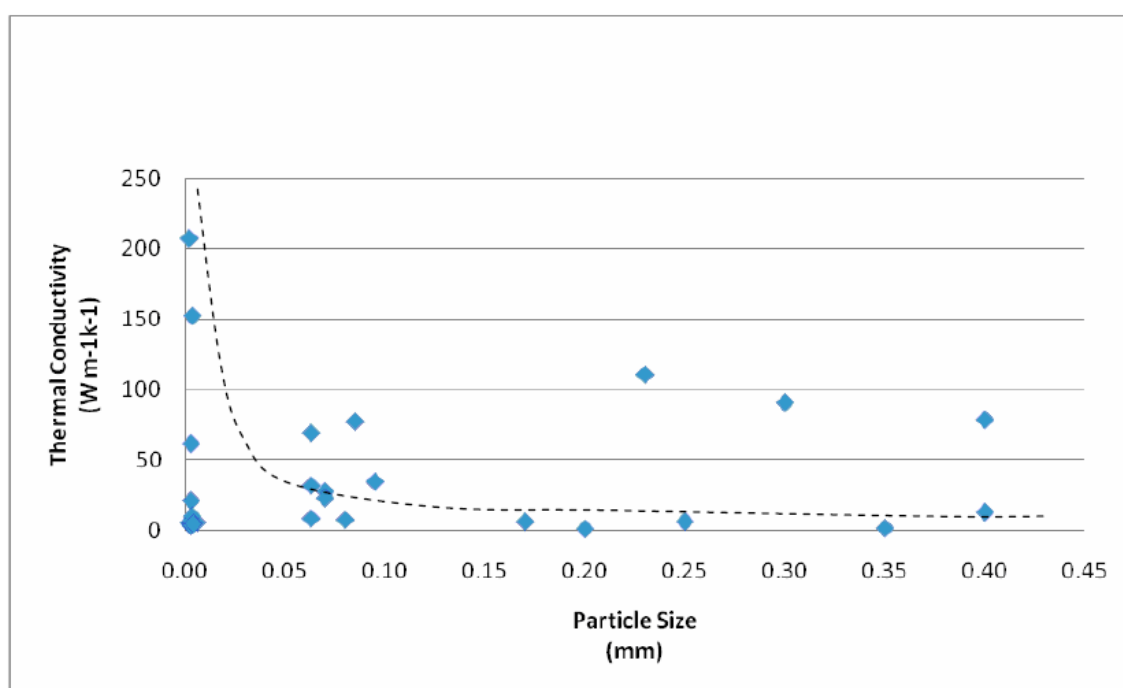


Fig 11: Graph showing the relationship between thermal conductivity and the particle size

CHAPTER 3: MATERIALS AND METHODS

3.1 WORK FLOW

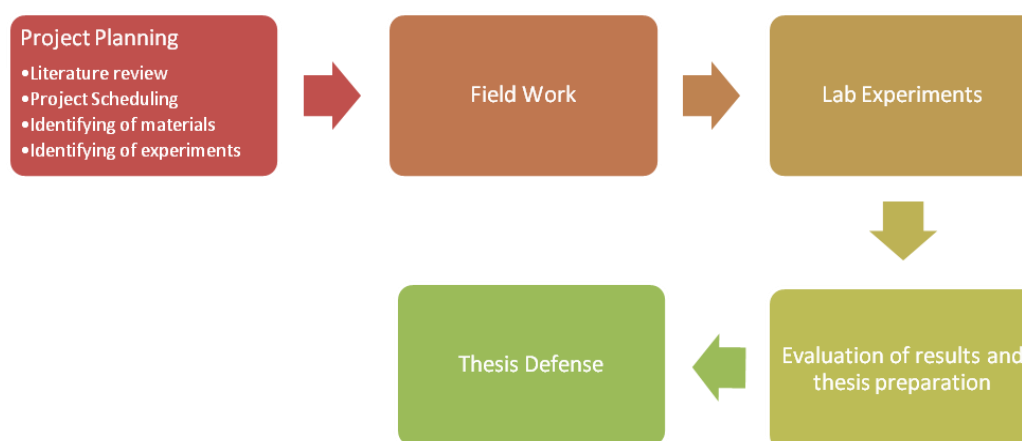


Fig 12: Work flow for FYP I & FYP II

3.2 STUDY AREA

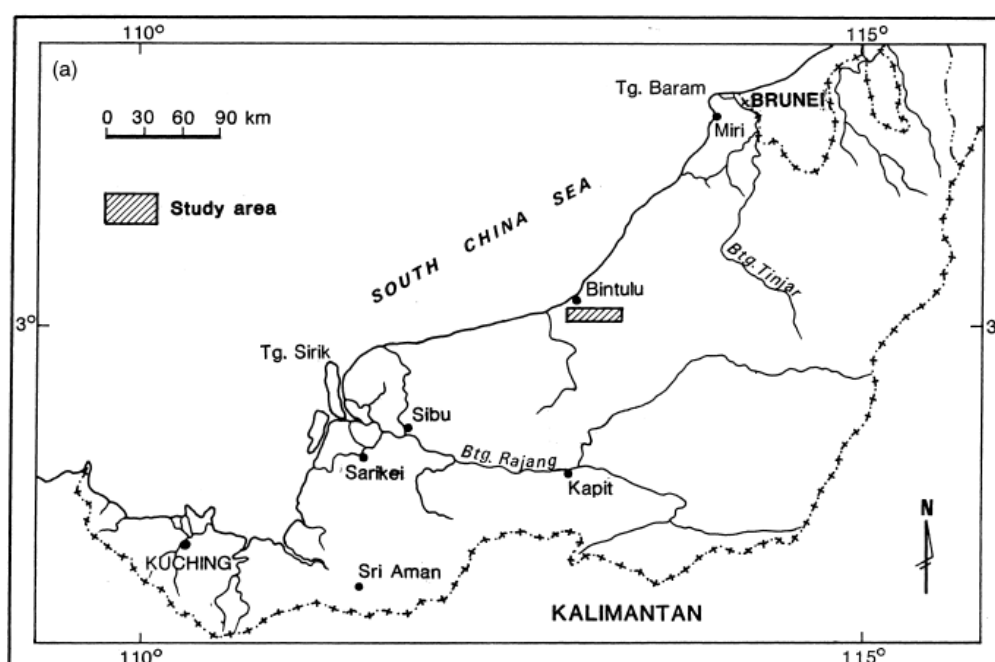


Fig 13: Location of the study area in Nyalau Formation

3.2.1 Outcrop 1

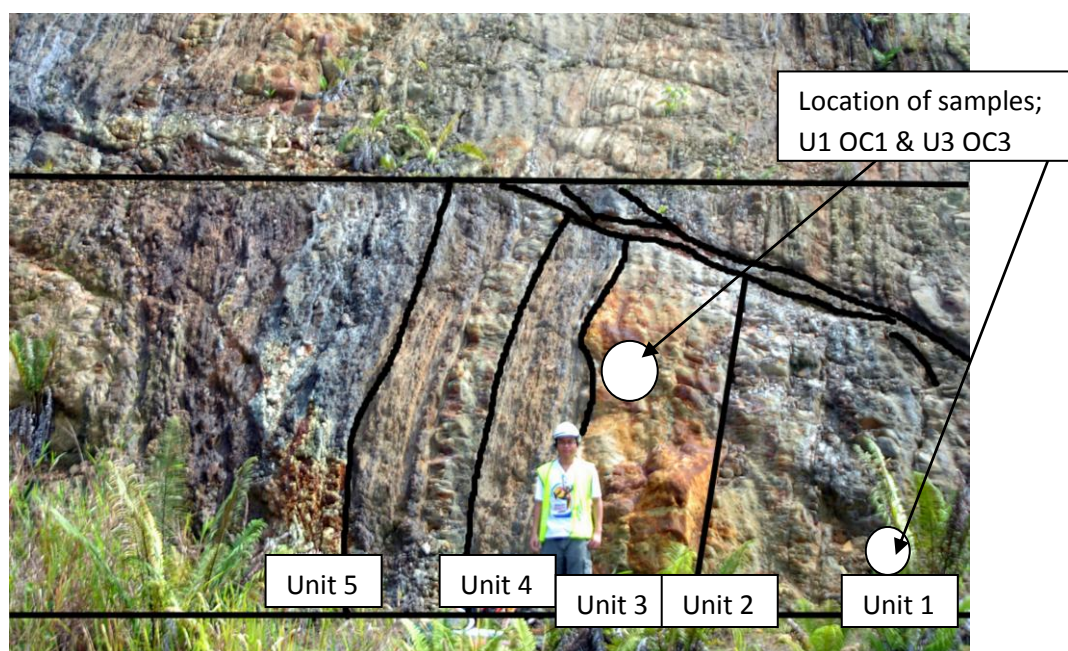


Figure 14: Unit 1 & Unit 3 of Outcrop 1

Position: N 02° 49' 53.7"

Elevation: 89ft above sea level

E 112° 54' 9.9"

3.2.2 Outcrop 2

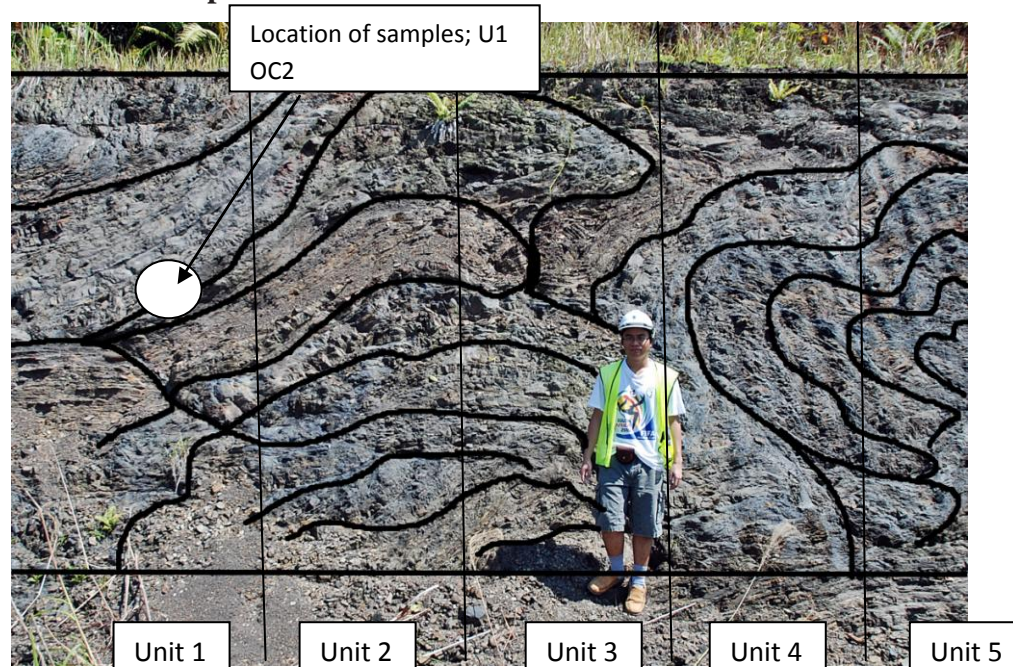


Figure 15: Unit 1 Outcrop 2

Position: N 02° 50' 56.9"

Elevation: 93 ft above sea level

E 112° 51' 50.9"

3.2.3 Outcrop 3

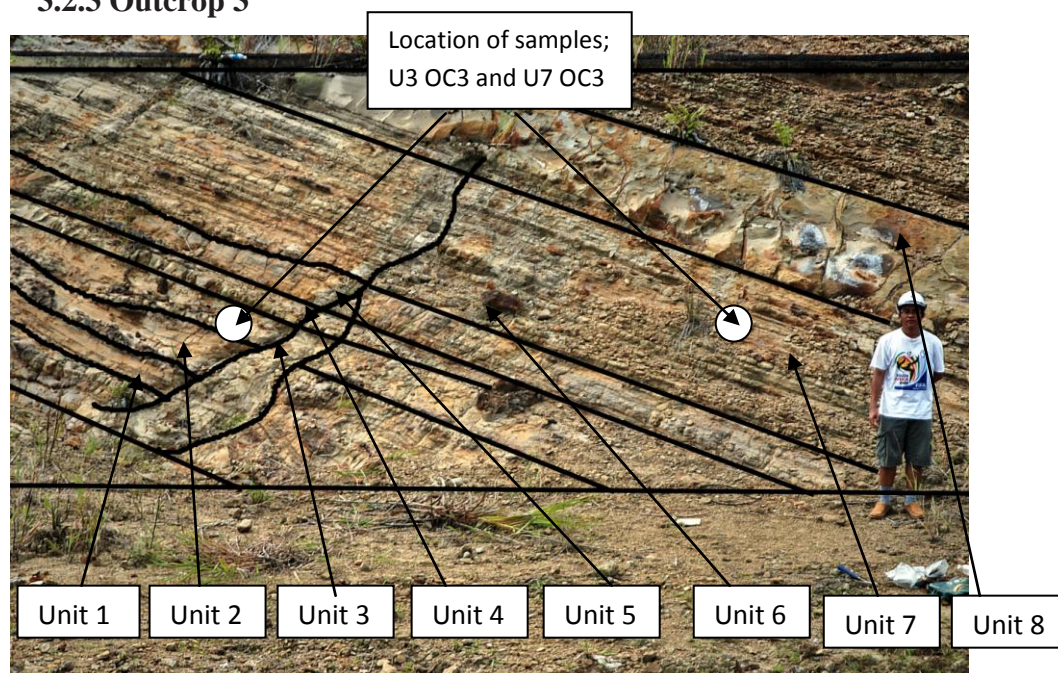


Figure 16: Unit 3 and Unit 7 of Outcrop 3

Position: N 03° 7' 28.8"

Elevation: 73ft from sea level

E 113° 2' 16.9"

3.3 RESEARCH METHODOLOGY

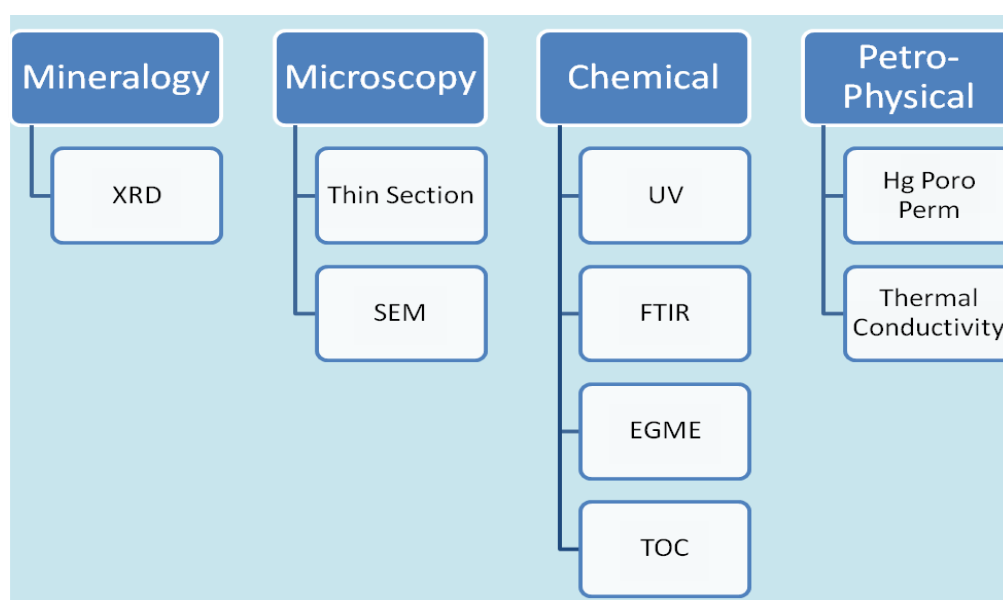


Figure 17: Laboratory experiment according to 4 categories (mineralogy, microscopy, chemical and petrophysical)

3.3.1 Mineralogy

In order to find and analyse the mineralogy of each samples, X-Ray Diffraction (XRD) experiment will be used. XRD is a lab method used in determines the mineral content by observing the scatters intensity of an X-ray beam hitting a sample, which reveals information such as crystallographic structure, chemical composition and physical properties of sample.

X-Ray Diffraction (XRD)

Chemicals and Apparatus

Sandstone sample (powder), Philips Xpert X-Ray Diffractometer

Procedure:

- The surface area was obtain using EGME method
- Samples were dried and place onto a slide
- Samples were then analysed using Philips Xpert X-Ray Diffractometer with $\text{CuK}\alpha$ radiation at scanning speed of $0.04^\circ/\text{s}$
- SPeaks obtained was identified using the database provided by International Centre for Diffraction Database (ICDD)

3.3.2 Microscopic

The microscopic properties is determined and analyzed by using two methods; Scanning Electron Microscope (SEM) and This Section. Both techniques involve observing by the naked eyes. The purpose of these experiments is to analyse the petrography descriptions, which is by observing and investigate the optical properties of the minerals in the rock. Among the petrography descriptions are field notes from the outcrop and megascopic description of samples. The detailed analysis of minerals structure and composition by thin-section and SEM method and the micro-texture and structure are critical to understand the origin and evolution of the parent rock.

Scanning Electron Microscope (SEM)

Chemicals and Apparatus

SEM machine, sandstone samples (rock chips)

Procedure:

- The rock chip samples are prepared onto a slide.
- The slide is placed into the SEM sample chamber
- SEM machine started and vacuum activated
- Images generated on the screen being taken based on the magnification
- A point of interest within the sample is chosen
- Images are captured by 500x, 1000x, 3000x, and 5000x
- Images are analysed for its mineral structure and composition

Thin Section

Chemicals and Apparatus

Sandstone samples (rock chip), hot plate, dyed resin, rock cutter, precision cutter, microscope

Procedure:

- A rock chip is cut off from the main samples by using a rock cutting machine.
- The rock chip is polished until it gets smooth area and left to dried on a hotplate (until all water is removed)
- Then, the rock chip is mixed with dyed resin until it gets harden inside. Leave it for few days.
- Then the sample is trimmed using precision cutter until it get a very flat surface, around 25-30 μ m.
- After that, sample is polished once more until the thickness is around 13 μ m. Sample is observed under a microscope until we get a clear view of grains.
- After confirming with the current view/surface of the sample, sample's picture is taken for analysis purpose.

3.3.3 Chemical Composition

To determine the chemical compositions, the experiments that will be used are X-Ray Fluorescence (XRF), Ultra Violet (UV), Fourier Transform Infrared Radiation (FTIR), EGME Test, and Total Organic Compound (TOC). All of these experiments are used to find and analyse the chemical composition in each samples. Examples chemical compositions that are usually found in (sedimentary) rocks are halite (rock salt), sylvite, barite and gypsum. The chemical analysis will help in determine the rock's origin, as well as the environment of deposition and crystal structures and necessary fabrics found in each samples.

Ultra Violet Visible Spectroscopy

Chemicals and Apparatus

Sandstone sample (liquid), Shimadzu UV Probe 2000 software, Shimadzu UV-3150 UV-VIS spectrophotometer, 0.5M hydrogen peroxide

Procedure:

- Powdered rocks were diluted in a test tube with 0.5M hydrogen peroxide and put to rest for a night.
- The extracted liquid was transferred in a quartz cuvette and analyzed using Shimadzu UV-3150 UV-VIS spectrophotometer.
- The spectrophotometer was set to acquire spectra in the range of 200-800nm with scanning interval of 0.5nm.
- The data acquired by the spectrophotometer was then viewed in Shimadzu UV Probe 2000 software to identify the spectral at 465nm and 665nm for determination of E4/E6 ratio.

Fourier Transform Infrared Radiation (FTIR)**Chemicals and Apparatus**

Sandstone samples (powder), Shimadzu 8400S FTIR, Shimadzu IRsolution software, Calcium Bromide

Procedure:

- Samples were prepared by pressing homogenous mixture of powdered samples (2mg) and KBr (100mg) into micro-disc pallet.
- These micro-disc pallets were then analyzed using a Shimadzu 8400S FTIR to determine the types of stretching bonds presence
- The spectroscope was set to Happ-Ganzel apodisation with resolution of 4.0 and to acquire wavelength in the range of 400-4000cm⁻¹.
- Shimadzu IRsolution software was used to view the acquired spectra from the spectroscope.
- Interpretation of functional groups from the spectra was made by comparing experimental values with available literatures (Schnitzer, 1982; Coates, 1996; Crews et al., 1998; Coates, 2000)

Ethylene Glycol Monomethyl Ether**Chemicals and Apparatus**

EGME solution, Calcium Chloride, rock samples (powder), oven, dry aluminium/glass tare, vacuum desiccator, plexiglass lid, weighting scales

Procedure:

Desiccant:

- Weight 120 grams of CaCl_2 into a 1-L beaker and dry in oven for an hour
- Weight 20 grams of EGME into 400mL beaker
- Remove CaCl_2 from oven and weight out 100 grams without cooling
- Add to the beaker containing EGME and mix immediately
- After solvate has cooled, place in a culture chamber and spread uniformly over bottom
- Store the culture chamber in sealed desiccators

Preparing the sample:

- 1 gram of oven dried soil passing a #40 sieve was placed in the bottom of a clean dry aluminium or glass tare.
- Mass of the soil to the nearest 0.001g is determined.
- A small pipette was used to place approximately 3mL of lab grade EGME over the soil.
- The soil and EGME were mixed together using a slow swirling motion until the mixture forms slurry and the appearance of the slurry is uniform.
- The tare was placed into vacuum desiccator and a small plexiglass lid is placed over the tare, leaving a gap of 2 to 3mm between the lid and tare.
- The lid of the desiccators was attached to a vacuum pump and evacuation process using vacuum began at least 635 mm Hg.
- After 12 – 16 hours, the tare was removed and the mass of the soil/EGME mixture was determined. This step is repeated approximately 24 hours.

Calculation:

- SSA is calculated as;

$SSA = W_a / 0.000286 W_s$, where;

SSA = Specific Surface Area in m^2/g

W_a = Weight of ethylene glycol mono ethyl ether (EGME) retained by the sample in grams (final slurry weight – W_s)

0.000286 = Weight of EGME required to form a monomolecular layer on a square meter of surface (g/m^2)

W_s = over dry weight of soil

Total Organic Compound

Chemicals and Apparatus

Sandstone samples (powder), O.I Analytical 1030S Solids TOC Module, small cup with quartz cotton in it, weighting scale

Procedure:

- Samples were dried
- Samples were prepared into a small cup with quartz cotton in it.
- Samples are weighted in the range between 100mg – 200mg.
- Then, samples were analysed using O.I Analytical 1030S Solids TOC Module.
- TOC value was obtained from IR detector at different temperature interval and displayed through WinTOC interface for data acquisition of analyzed samples.
- Classifications of organic carbon content were made based on the descriptions given by Tissot & Welte (1984).

3.3.4 Petrophysical

Petrophysical means the study of physical and chemical properties that describe the occurrence and behaviour of rocks. Some of the key properties that will be studied are lithology, porosity, permeability, density and thermal conductivity. In this section, the sample's petrophysical properties are studied by two methods; Hg Poro-Perm and thermal conductivity.

Hg Porosimeter

Chemicals and Apparatus

Sandstone samples (rock chip), Pascal 240 Thermal Fisher Mercury Intrusion Porosimeter, weighting scale

Procedure:

- Samples are dried
- Samples were cut using a small-sized bow saw into a known dimension and weighed (1cm x 1cm x 1cm) before being analyzed with Pascal 240 Thermo Fischer Mercury Intrusion Porosimeter.
- Samples were weighted in air and in water to obtain density.
- Samples were first degassed and then intruded by Hg.
- Apparent density, bulk density, porosity and open pore size distribution (pore diameter between 3.7 and 58000 nm) of each sample have been computed using the PASCAL (Pressurization with Automatic Speed-up by Continuous Adjustment Logic) method.

Thermal Conductivity

Chemicals and Apparatus

Thermometer with 2 probes, rock samples, stopwatch, heating pad

Procedure:

- A sample of rock was prepared, then, the heat flowing position was determined onto the rock. 3 lines being drawn (Point A & Point B), each end by end on the rock. Each lines is 10 cm
- Step 1 repeated for each surface of the rock (front and back). Named as Face A and Face B.
- The two probes (thermometer) for T_1 was placed at Point A while T_2 was placed on Point B
- Surface area value of the rock for heating source purpose was taken.
- Heating pad was placed onto the surface area of the rock in which the heat will enter and flow into the rock.
- Initial reading taken for T_1 and T_2 .
- Stopwatch started. For every 1 minute, reading of T_1 and T_2 were taken down. Process repeated every 1 minute for 30 minutes.
- Step 1 to 7 was repeated with the next line (the rock is made sure to be cooled down fully before proceed with the next lines).
- Data of the thermal reading was key-in into thermal excel.
- From the data in thermal excel, graphs were being plotted by Delta T, in °C (Difference temperature between T_1 and T_2) vs Time, in minute
- Thermal conductivity value, k, are calculated using equation found in the thermal table.

3.4 PROJECT ACTIVITIES

Among the project activities that will be conducted during Final Year Project II period are;

- Conduct research onto mineralogy and microscopy, potential reservoir quality rocks in Sarawak and related case study
- Acquiring geological data from previous research of Nyalau Formation
- Conduct observation and examination (lithofacies, formation structure) onto the Nyalau Formation and samples of sedimentary rocks
- Conduct laboratory experiments and analysis of data acquired
- Discussion on data acquired and suggests improvement in research and discussion

3.5 KEY MILESTONE

Week 1 – 13: Continue works from FYP I

Week 8: Submission of Progress Report

Week 10: Pre-SEDEX combined with seminar/poster submission

Week 12: Submission of Final Report

Week 14: Final Oral Presentation

Week 15: Submission of Hardbound copy

CHAPTER 4: RESULTS & DISCUSSIONS

Below are the summaries of the results obtained from each experiment phases;

4.1 THERMAL CONDUCTIVITY

Graphs for thermal conductivity, k can be refer to Appendix 4

Thermal Conductivity, k for Face A (weathered/outer surface) and Face B (inner surface) of the rock samples are as below;

Sample	Face A
U1 OC1	$1.71 \text{ W m}^{-1} \text{ K}^{-1}$
U3 OC1	$1.59 \text{ W m}^{-1} \text{ K}^{-1}$
U1 OC2	$1.65 \text{ W m}^{-1} \text{ K}^{-1}$
U3 OC3	$7.51 \text{ W m}^{-1} \text{ K}^{-1}$
U7 OC3	$7.85 \text{ W m}^{-1} \text{ K}^{-1}$

Table 2: Weathered Surfaces

Sample	Face B
U1 OC1	$2.27 \text{ W m}^{-1} \text{ K}^{-1}$
U3 OC1	$3.23 \text{ W m}^{-1} \text{ K}^{-1}$
U1 OC2	$1.69 \text{ W m}^{-1} \text{ K}^{-1}$
U3 OC3	$8.52 \text{ W m}^{-1} \text{ K}^{-1}$
U7 OC3	$7.39 \text{ W m}^{-1} \text{ K}^{-1}$

Table 3: Inner Surfaces

Unit for $k = \text{W m}^{-1} \text{ K}^{-1}$

Based on the results, most of the thermal conductivity within each samples are within the range of $1 - 10 \text{ W m}^{-1} \text{ K}^{-1}$. High thermal conductivity indicates that the sample could have small particle size and high grains contact. The other samples with low thermal conductivity indicated larger particle size and low grains contact as well as the matrix size, which might be filled with air or fluid with different heat conductivity. But since the rock are not homogeneous in terms of mineralogy, the minerals can also influence thermal conductivity. For example, the existance of quartz since quartz usually have high thermal conductivity compare to clay minerals. Iron oxide existance also affects the thermal conductivity. Overall, the thermal conductivity coefficient is;

Sample	Face A
U1 OC1	1.99 W m ⁻¹ K ⁻¹
U3 OC1	2.41 W m ⁻¹ K ⁻¹
U1 OC2	1.67 W m ⁻¹ K ⁻¹
U3 OC3	8.02 W m ⁻¹ K ⁻¹
U7 OC3	7.64 W m ⁻¹ K ⁻¹

Table 4: Overall Thermal Conductivity Coefficient

Outcrop 2 have the smallest thermal conductivity coefficient while outcrop 3 have the highest thermal conductivity coiefficient.

4.2 FOURIER TRANSFORM INFRARED RADIATION

Graphs for FTIR can be refer to Appendix 5

Functional Group	Wavelength (cm ⁻¹)	Type of Vibration
Aryl C=C	472	Ring bend
Aryl C=C	528.55	Ring bend
CH=CH	694.48	C-H out-of-plane bend
C≡C-H	778.96	C-H bend
Aryl-H	1030.8	In-plane bend
C=CH ₂	1416.97	C-H in-plane bend
C=C	1637.48	C=C str
C=N=N	2030.08	Asym str
O-H	3425.25	str

Table 5: U1 OC1

Based on the result, the aromatic functional group; Aryl C=C can be found on wavelength 472cm⁻¹ and 528.55cm⁻¹ as type of vibration is ring bend. The aromatic functional group; Aryl-H can be found at 1030cm⁻¹ with type of vibration is in-plane bend. The CH=CH can be found on wavelength 694.48cm⁻¹ with type of vibration is C-H out-of-plane bend. The C≡C-H compound can be found at wavelength 778.96cm⁻¹ with type of vibration is C-H bend. The C=CH₂ compound can be found at wavelength 1416.97cm⁻¹ with type of vibration is C-H in-plane bend. The C=C compound can be found at wavelength of 1637.48cm⁻¹ with type of vibration is C=C str. The C=N=N is found at 2030.08cm⁻¹ with type of vibration is asym str. Finally

O-H (free) functional group can be found at wavelength 3425.25cm^{-1} with as type of vibration is str.

Functional Group	Wavelength (cm-1)	Type of Vibration
Aryl C=C	471.65	Ring bend
Aryl C=C	529.62	Ring bend
CH=CH	694.24	C-H out-of-plane bend
C≡C-H	778.82	C-H bend
C≡C-H	797.45	C-H bend
Aryl-H	1030.64	In-plane bend
C=CH ₂	1417	C-H in-plane bend
C=C	1637.86	C=C str
C=N=N	2030.47	Asym str
O-H	3434.52	Str

Table 6: U3 OC1

Based on the result, the aromatic functional group; Aryl C=C can be found on wavelength 471.65cm^{-1} and 529.62cm^{-1} as the type of vibration is ring bend. The aromatic functional group; Aryl-H can be found at 1030.64cm^{-1} with type of vibration is in-plane bend. The CH=CH can be found on wavelength 694.24cm^{-1} with type of vibration is C-H out-of-plane bend. The C≡C-H can be found at wavelength 778.82cm^{-1} and 797.45cm^{-1} with type of vibration is C-H bend. The C=CH₂ can be found at wavelength 1417cm^{-1} with type of vibration is C-H in-plane bend. The C=C compound can be found at wavelength of 1637.86cm^{-1} with type of vibration is C=C str. The C=N=N is found at 2030.47cm^{-1} with type of vibration is asym str. Finally O-H (free) functional group can be found at wavelength 3425.25cm^{-1} with as type of vibration is str.

Functional Group	Wavelength (cm^{-1})	Type of Vibration
Aryl C=C	470.94	Ring bend
Aryl C=C	534.95	Ring bend
CH=CH	694.26	C-H out-of-plane bend
Aryl-H	778.53	In-plane bend
Aryl-H	797.01	In-plane bend
C \equiv C-H	913.1	C-H bend
Aryl-H	1008.51	In-plane bend
Aryl-H	1032.22	In-plane bend
C=C	1637.44	C=C str.
C=C=CH ₂	1870.39	C=C=C asym str.
O-H	3447.89	Str.
O-H	3619.97	Str.
O-H	3698.81	Str.

Table 7: U1 OC2

Based on the result, the aromatic functional group; Aryl C=C can be found on wavelength 470.94cm^{-1} and 534.95cm^{-1} as the type of vibration is ring bend. The aromatic functional group; Aryl-H can be found at 778.53cm^{-1} , 797.01cm^{-1} , 1008.51cm^{-1} and 1032.22cm^{-1} with type of vibration is in-plane bend. The CH=CH can be found on wavelength 694.26cm^{-1} with type of vibration is C-H out-of-plane bend. The C \equiv C-H can be found at wavelength 913.10cm^{-1} with type of vibration is C-H bend. The C=C=CH₂ can be found at wavelength 1870.39cm^{-1} with type of vibration is C=C=C asym str. The C=C can be found at wavelength of 1637.44cm^{-1} with type of vibration is C=C str. Finally O-H (free) functional group can be found at wavelength 3447.89cm^{-1} , 3619.97cm^{-1} and 3698.81cm^{-1} with type of vibration is str.

Functional Group	Wavelength (cm^{-1})	Type of Vibration
Aryl C=C	471.48	Ring bend
Aryl C=C	533.4	Ring bend
Aryl-H	694.3	In-plane bend
Aryl-H	778.92	In-plane bend
Aryl-H	797.91	In-plane bend
Aryl-H	1031.69	In-plane bend
CH ₂	1416.86	Str.
Aryl C=C	1551.91	Ring bend
C=C	1638.01	C=C str.
C=N=N	2030.29	Asym str.
O-H	3434.69	Str.

Table 8: U3 OC3

Based on the result, the aromatic functional group; Aryl C=C can be found on wavelength 471.48cm^{-1} , 533.4cm^{-1} and 1551.91cm^{-1} as the type of vibration is ring bend. The aromatic functional group; Aryl-H can be found at 694.3cm^{-1} , 778.92cm^{-1} , 797.91cm^{-1} and 1031.69cm^{-1} with type of vibration is in-plane bend. The CH₂ can be found on wavelength 1416.86cm^{-1} with type of vibration is str. The C=C can be found at wavelength 1638.01cm^{-1} with type of vibration is C=C str. The C=N=N can be found at wavelength 2030.29cm^{-1} with type of vibration is asym str. Finally, the O-H (free) functional group can be found at wavelength 3434.69cm^{-1} with type of vibration is str.

Functional Group	Wavelength (cm^{-1})	Type of Vibration
Aryl C=C	471.04	Ring bend
Aryl C=C	534.26	Ring bend
Aryl-H	694.45	In-plane bend
Aryl-H	778.85	In-plane bend
Aryl-H	797.63	In-plane bend
C \equiv C-H	914.47	C-H bend
Aryl-H	1031.9	In-plane bend
CH ₂	1416.48	Str.
Aryl C=C	1552.38	Ring bend
C=C	1634.28	C=C str.
C=N=N	2009.49	Asym str.
OH	3434.26	Str.

Table 9: U7 OC3

Based on the result, the aromatic functional group; Aryl C=C can be found on wavelength 471.04cm^{-1} , 534.26cm^{-1} and 1551.38cm^{-1} as the type of vibration is ring bend. The aromatic functional group; Aryl-H can be found at 694.45cm^{-1} , 778.85cm^{-1} , 797.63cm^{-1} and 1031.9cm^{-1} with type of vibration is in-plane bend. The C \equiv C-H can be found on wavelength 914.47cm^{-1} with type of vibration is C-H bend. The CH₂ can be found at wavelength 1416.48cm^{-1} with type of vibration is str. The C=C can be found at wavelength 1634.28cm^{-1} with type of vibration is C=C str. The C=N=N is found at 2009.49cm^{-1} with type of vibration is asym str. Finally, the O-H (free) functional group can be found at wavelength 3434.26cm^{-1} with type of vibration is str.

4.3 ULTRAVIOLET

Full table can be refer at Appendix 6

Ultraviolet is part of the mineralogy test. Its main purpose is to find the ratio of humic acid to fulvic acid. Humic acid is a component of humic substance, which is a major organic constituent of soil (humus), peat, coal and many upland streams. Fulvic acids are humic acids of lower molecular weight and higher oxygen content than other humic acid. Humic acid shows aromatic compound while fulvic acid shows aliphatic compound.

Humic acid has the average chemical formula $C_{187}H_{186}O_{89}N_9S_1$ and is insoluble in strong acid ($pH = 1$). A 1:1 hydrogen-to-carbon ratio indicates a significant degree of aromatic character (i.e., the presence of benzene rings in the structure). Fulvic acid is soluble in strong acid ($pH = 1$) and has the average chemical formula $C_{135}H_{182}O_{95}N_5S_2$. A hydrogen-to-carbon ratio greater than 1:1 indicates less aromatic character (i.e., fewer benzene rings in the structure).

From this experiment, full data can be referred to Appendix 4 we observe the wavelength at E4 which is at 465nm to identify the value of humic acid while E6 which is at 665nm, for fulvic acid. The ratio can be found by finding the adsorption of UV during 465nm and 665 nm. Below is the result for each sample; [Calculation: Ratio = E4/E6]

Samples	U1 OC1	U3 OC1	U1 OC2	U3 OC3	U7 OC3
Ratio	1.20	1.20	1.25	1.17	1.23

Table 10: E4/E6 ratio

Based on the results, U1 OC2 shows the highest E4/E6 ratio while U3 OC3 shows the lowest E4/E6 ratio. Thus, U1 OC2 has the highest degree of condensation of aromatic network of humic structures while U3 OC3 has the lowest E4/E6 ratio

4.4 X-RAY DIFFRACTION

Graphs can be refer to Appendix 7

X-Ray Diffraction test is used to identify the mineral(s) content found in the sandstone samples. Results in graphs were obtained and the Speaks were identified using the database provided by International Centre for Diffraction Database (ICDD). Minerals found in each sandstone samples are;

Samples	U1 OC1	U3 OC1	U1 OC2	U3 OC3	U7 OC3
Minerals	<ul style="list-style-type: none"> • Quartz • Albite • Siderite • Muscovite • Dolomite • Hematite 	<ul style="list-style-type: none"> • Quartz • Muscovite • Albite • Pyrite • Hematite • Siderite • Dolomite 	<ul style="list-style-type: none"> • Quartz • Pyrite • Aragonite • Siderite • Hematite • Dolomite 	<ul style="list-style-type: none"> • Quartz • Albite • Pyrite • Siderite • Muscovite • Hematite • Dolomite 	<ul style="list-style-type: none"> • Quartz • Albite • Siderite • Muscovite • Pyrite • Hematite • Dolomite

Table 11: XRD results

Mineral(s) Description:

Carbonate mineral;

- **Quartz** – The most common minerals in the earth's crust. It is made up of a continuous framework of SiO_4 silicon–oxygen tetrahedra, with each oxygen being shared between two tetrahedra, giving an overall formula SiO_2 (silicon oxide). Usually pure, coarse grained with cross bedding.
- **Aragonite** - one of the two common, naturally occurring, crystal forms of calcium carbonate, CaCO_3 (the other form being the mineral calcite). It is formed by biological and physical processes, including precipitation from marine and freshwater environments.

Feldspar;

- **Albite** - It is felsic plagioclase feldspar mineral. Feldspar is also commonly found in sandstone, Albite is considered parts of minerals in sandstone. Its chemical composition is $\text{NaAlSi}_3\text{O}_8$. Usually pure white in color.
- **Dolomite** – It is feldspar mineral composed of calcium magnesium carbonate $\text{CaMg}(\text{CO}_3)_2$. The term is also used to describe the sedimentary carbonate rock dolostone. The mineral dolomite crystallizes in the trigonal-rhombohedral system. It forms white, gray to pink, commonly curved (saddle shape) crystals. It is usually found in dolomite rock or limestone. Also occasionally in high-temperature metamorphic rocks and low-temperature hydrothermal veins.
- **Siderite** - It is commonly found in hydrothermal veins, and is associated with barite, fluorite, galena, and others. It is also a common diagenetic mineral in shales and sandstones, where it sometimes forms concretions. Siderite commonly forms in primarily bedded, biosedimentary deposits, also in metamorphic and igneous rocks. Forms a series with rhochrosite.
- **Hematite** - Hematite is one of the most common minerals. The color of most red and brown rock, such as sandstone, is caused by small amounts of Hematite. It is also be responsible for the red color of many minerals such as Garnet. Its formula is Fe_2O_3 . It also contains iron oxide, and possible titanium.

- **Pyrite** –It is an iron sulfide with the formula FeS_2 . Pyrite is also usually found associated with other sulfides or oxides in quartz veins, sedimentary rock, and metamorphic rock, as well as in coal beds, and as a replacement mineral in fossils. It is pale brass-yellow, tarnishes darker and iridescent in colour

Clay mineral;

- **Muscovite** – Muscovite is a type of clay mineral found in sandstone. It is also known as common mica. Its formula is $\text{KAl}_2(\text{AlSi}_3\text{O}_{10})(\text{OH})_2$. It can be from white to colorless. Its crystal system is monoclinic

4.5 ETHYLENE GLYCOL MONOETHYL ETHER

Surface area determines many physical and chemical properties of materials. Water retention and movement, cation exchange capacity, pesticide adsorption, and biological processes are closely related to specific surface. Samples vary widely in their reactive surface area because of difference in organic composition, mineralogy and in their particle size distribution (Carter et al, 1986). Specific surface, defines as surface area per unit mass of sample, is express in units of m^2/g or cm^2/g . Below are the results of specific surface obtain from each outcrops in Sarawak;

Samples	U1 OC1	U3 OC1	U1 OC2	U3 OC3	U7 OC3
SSA (m^2/g)	27	21	9	33	21

Table 12: EGME Results

Based on the results, U3 OC3 has the largest specific surface area, which is $33\text{m}^2/\text{g}$ while the lowest specific surface area is U1 OC2, which is $9\text{m}^2/\text{g}$. Averagely, outcrop OC3 has biggest surface area, means more reaction could happen onto the surface compare to other outcrops.

4.6 TOTAL ORGANIC CARBON

Total organic carbon is the amount of carbon bound in organic compounds that are found in the outcrops. The results/concentrations obtain from TOC experiment will help to indicate the amount of organic carbon found and possibly deduced the occurrence of organic compound that have been accumulated in the outcrops. Below are the results;

Samples	U1 OC1	U3 OC1	U1 OC2	U3 OC3	U7 OC3
Concentration (%)	0	1.23	0.23	1.18	1.17

Table 13: TOC Results

Based on the results, U3 OC1 has the highest concentration of TOC while U1 OC1 has no concentration of TOC. But majority of the outcrops have very low concentration of TOC (0% – 1.3%). OC1 and OC2 are located in the deeper parts of Sarawak, which means there is less organic compound accumulated there, while OC3 is located near coastal area off Bintulu (Sarawak), meaning much more organic compound accumulated there.

4.7 Hg POROSIMETER

Porosity plays an important part of the microscopy of sedimentary rocks. This parameter will influence the characteristic of the outcrops. For example, thermal conductivity. High porosity causes lower thermal conductivity because of air and other fluids like water infill the pores of the rock compared to the mineral and vice versa (Padmanabhan et al, 2010). Below are the results for porosity;

Samples	U1 OC1	U3 OC1	U1 OC2	U3 OC3	U7 OC3
Porosity (%)	14.01	19.27	25.80	28.34	37.71

Table 14: Hg Porosimeter Results

Based on the results, U7 OC3 yields the highest porosity value, which is 37.71%, while U1 OC1 yields the lowest porosity value, which is 14.01%. Overall, the outcrop 3 has the highest porosity while outcrop 1 has the lowest porosity. Porosity values is increasing from outcrop 3 to outcrop 2 and eventually to outcrop 1, which have shown that each outcrops in Nyalau Formation have variety types of grain sizes, pore distributions as well as particle arrangements. (Hutchinson et al, 1997) From this experiment, the porosity value are measured based upon the pore size distribution within each samples using mercury intrusion. Further explanations regarding the pore size distribution are explained below;

4.7.1 Pore Size Distribution

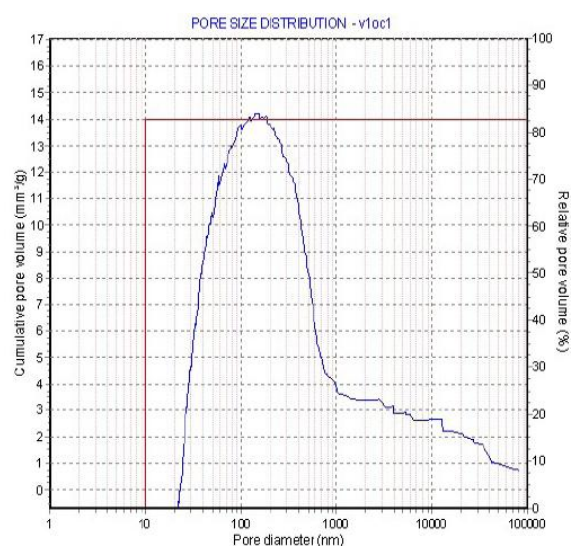


Figure 18: U1 OC1

80% of the porosity that comes from pore diameter (pore size) ranging from 20 – 1000nm while 20% represented the range of 1001 – 100000nm. This percentage of porosity that covered the samples represents the 14.01% of ‘total’ porosity value within the sample.

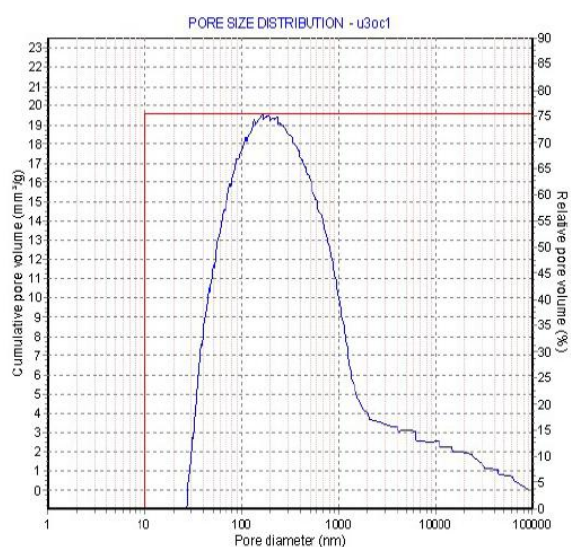


Figure 19: U3 OC1

85% of the porosity that comes from pore diameter (pore size) ranging from 18 – 1100nm while 15% represented the range of 1101 – 100000nm. This percentage of

porosity that covered the samples represents the 19.27% of ‘total’ porosity value within the sample.

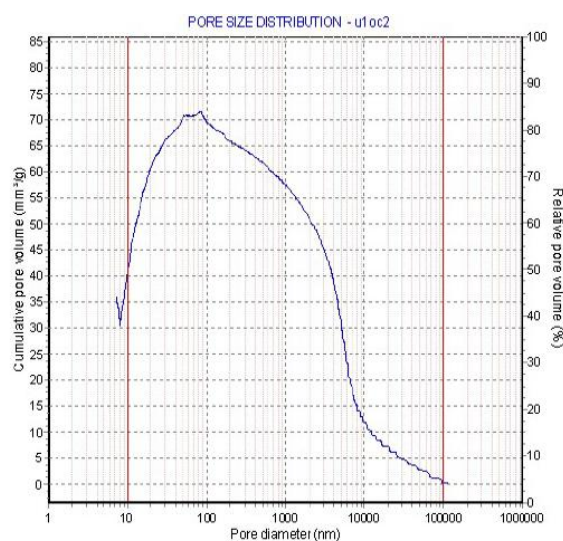


Figure 20: U1 OC2

90% of the porosity that comes from pore diameter (pore size) ranging from 8 – 1500nm while 10% represented the range of 1501 – 100000nm. This percentage of porosity that covered the samples represents the 25.80% of ‘total’ porosity value within the sample.

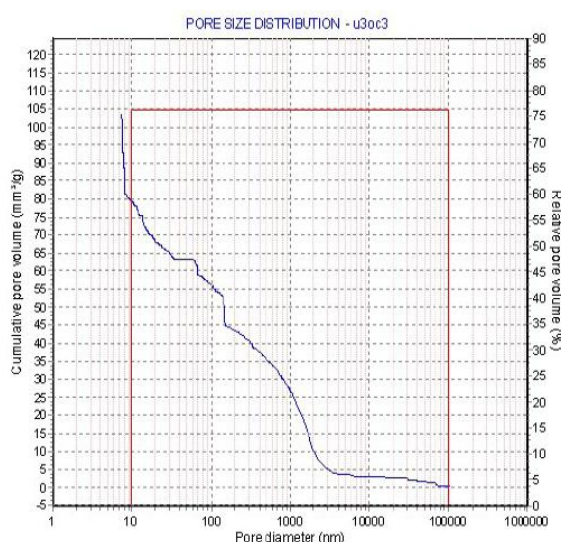


Figure 21: U3 OC3

95% of the porosity that comes from pore diameter (pore size) ranging from 8 – 1200nm while 5% represented the range of 1201 – 100000nm. This percentage of porosity that covered the samples represents the 28.34% of ‘total’ porosity value within the sample.

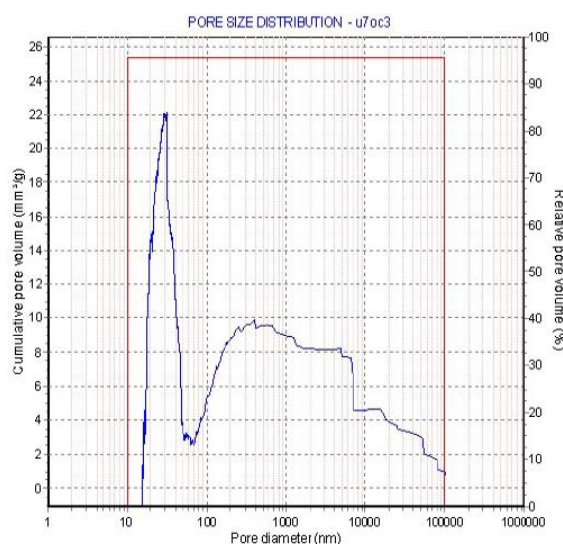


Figure 22: U7 OC3

15% of the porosity that comes from pore diameter (pore size) ranging from 10.7 – 16nm while 85% represented the range of 17 – 100000nm. This percentage of porosity that covered the samples represents the 37.71% of ‘total’ porosity value within the sample.

4.8 SCANNING ELECTRON MICROSCOPE

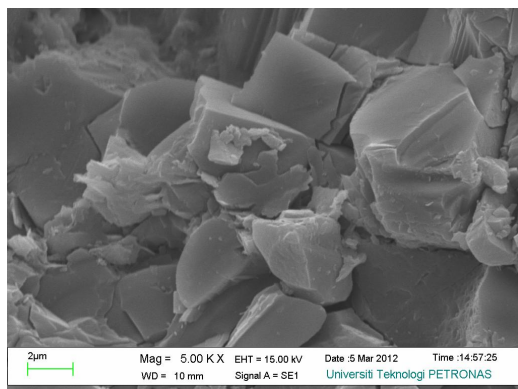


Figure 23: U1 OC1

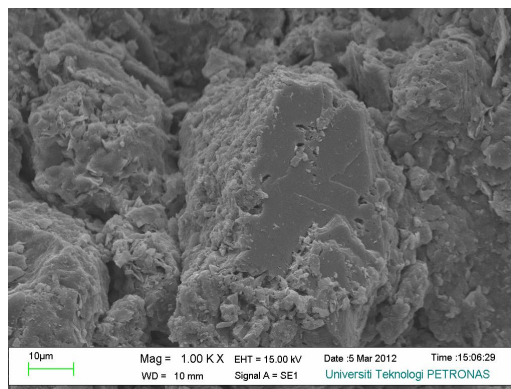


Figure 24: U3 OC1

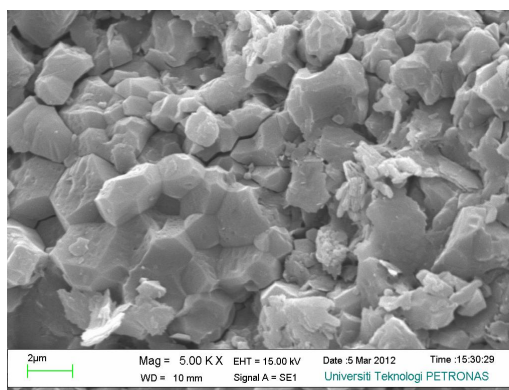


Figure 25: U1 OC2

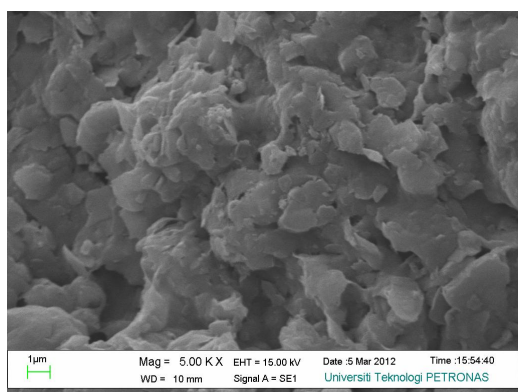


Figure 26: U3 OC3

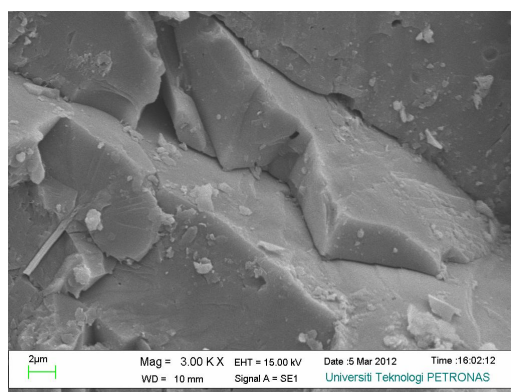


Figure 27: U7 OC3

Pictures of samples are taken based upon the majority of the types of grains that appear in the sandstone samples. Magnification is 5000x. Below are the discussions;

U1 OC1:

- Square-shape quartz surrounded by flaky clay mineral such as muscovite.

U3 OC1

- Thin shape quartz surrounded by flaky clay minerals such as muscovite
- Flaky shape feldspar existed, surrounding quartz mineral.

U1 OC2

- Detrital quartz grain with four slightly concave surrounded by carbonate mineral such as aragonite.
- Feldspar existed around the quartz mineral.

U3 OC3

- Detrital quartz grain with inter-connected four slightly concave surrounded by flaky clay mineral such as muscovite.

U7 OC3

- Clear looking rectangular shape quartz.

4.9 THIN SECTION

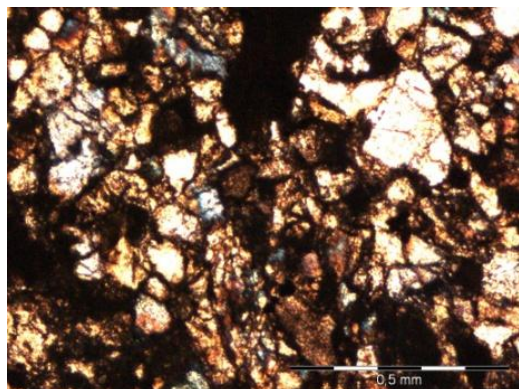


Figure 28: U1 OC1

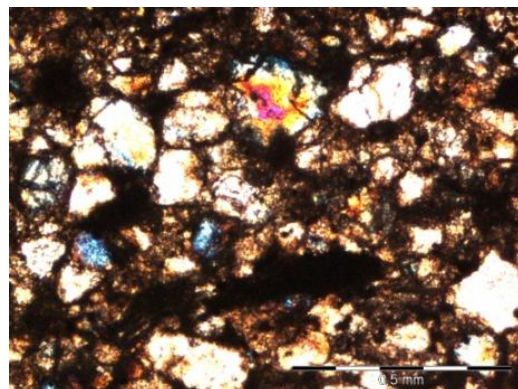


Figure 29: U3 OC1

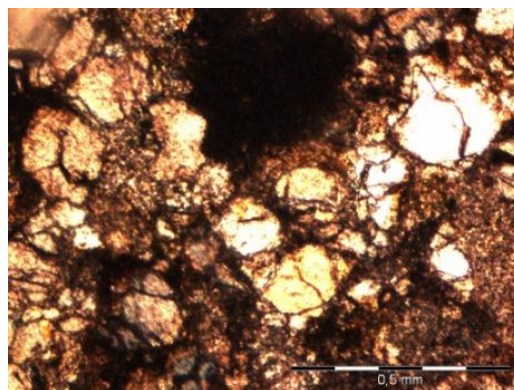


Figure 30: U1 OC2

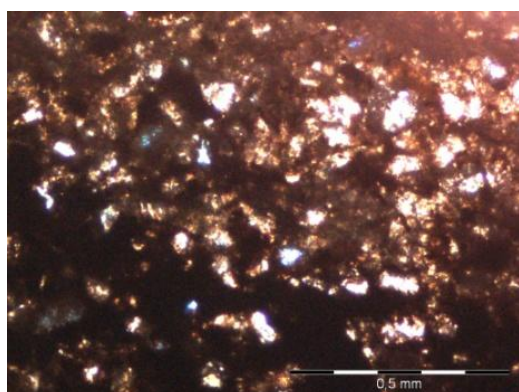


Figure 31: U1 OC1

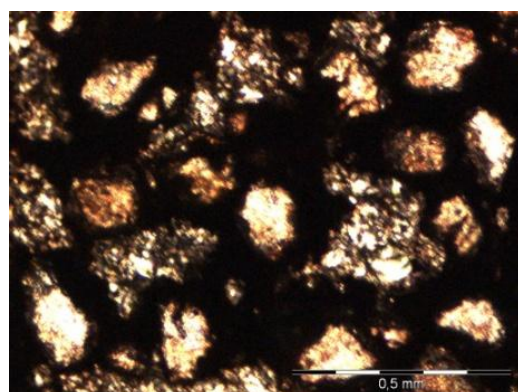


Figure 32: U3 OC1

Pictures of samples are taken based upon the majority of the types of grains that appear in the sandstone samples. Below are the discussions;

U1 OC1

- Quartz grain are displayed
- Grains are closed to each other, relatively 0.3mm – 0.5mm
- The matrix is small, which means the pores are relatively small
- Particle distribution is un-uniform
- Very few feldspathic grain indication

U3 OC1

- Quartz grain are displayed
- Grains are closed to each other, relatively more than 0.5mm
- The matrix is medium size, which means the pores are relatively medium.
- Particle distribution is un-uniform
- Very few feldspathic grain indication

U1 OC2

- The brown coloured grain suggest it may be sort of iron oxide mineral as well as indication coarse feldspathic sandstone
- Grains are closed to each other, relatively 0.5mm – 1.0mm
- The matrix size is large, which means the pores are relatively large.
- Particles distribution is uniform

U3 OC3

- Quartz grain are displayed
- Grains are disperse among each other, with size relatively less than 0.25mm
- The matrix size is large, which means the pores are relatively large.
- Particles distribution is un-uniform
- Very few feldspathic grain indication

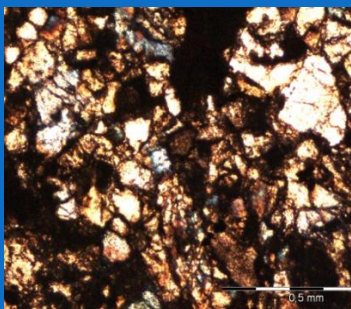
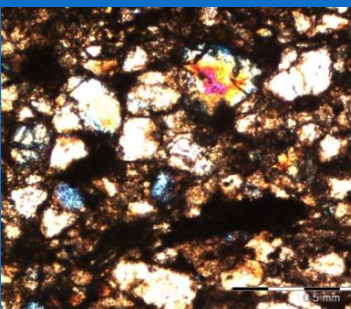
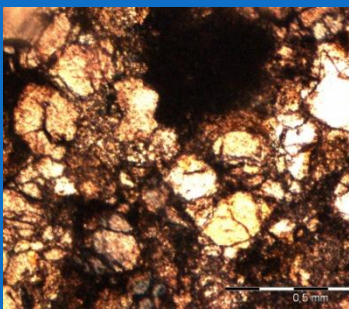
U7 OC3

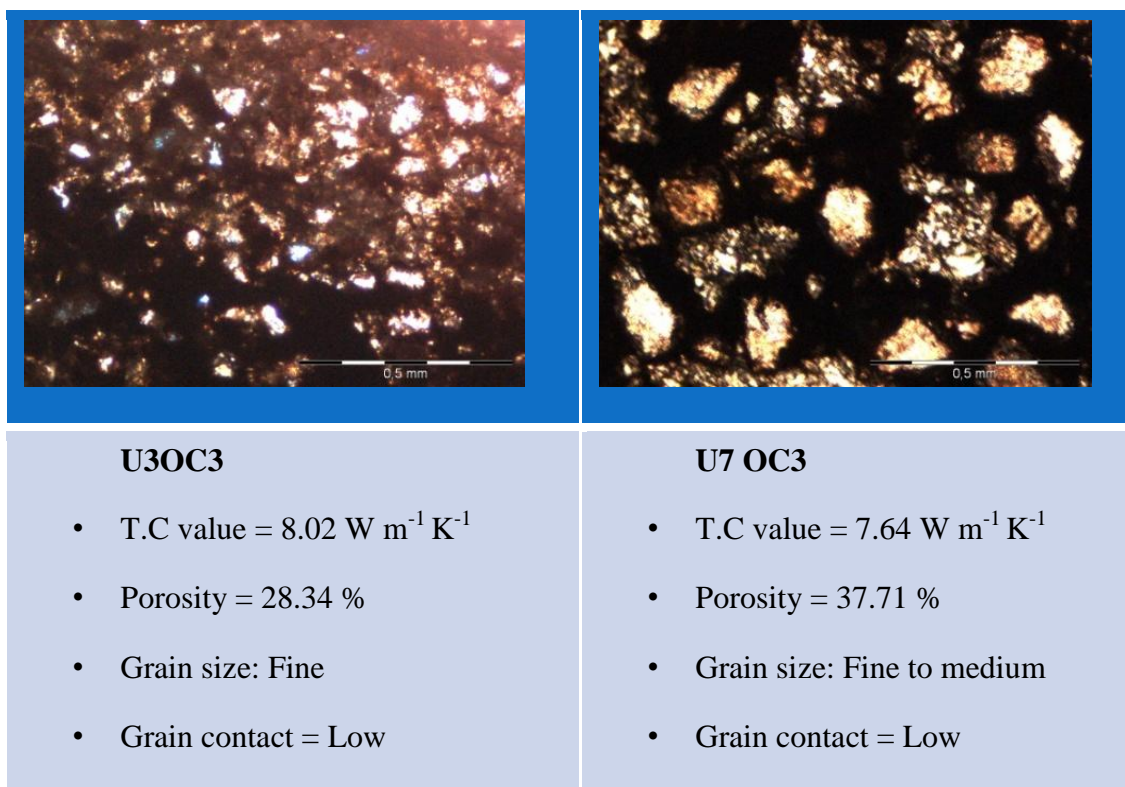
- Quartz grain are displayed
- Grains are disperse among each other, with size relatively 0.5mm – 1.0mm
- Grains have pores in it (observed from the cracked in it)

- The matrix size is large, which means the pores are relatively large.
- Particle distribution is uniform.

4.10 EVALUATION OF FABRIC VARIABILITY ONTO PETROPHYSICAL PROPERTIES

4.10.1 Fabric variability and petrophysical properties onto Thin Section

		
<p>U1 OC1</p> <ul style="list-style-type: none"> • T.C value = 1.99 $\text{W m}^{-1} \text{K}^{-1}$ • Porosity = 14.01 % • Grain size: Medium • Grain contact = High 	<p>U3 OC1</p> <ul style="list-style-type: none"> • T.C value = 2.41 $\text{W m}^{-1} \text{K}^{-1}$ • Porosity = 19.27 % • Grain size: Medium • Grain contact = High 	<ul style="list-style-type: none"> • U1 OC2 • T.C value = 1.67 $\text{W m}^{-1} \text{K}^{-1}$ • Porosity = 25.80 % • Grain size: Coarse • Grain contact = High



4.10.2 Thermal Conductivity vs Total Organic Carbon

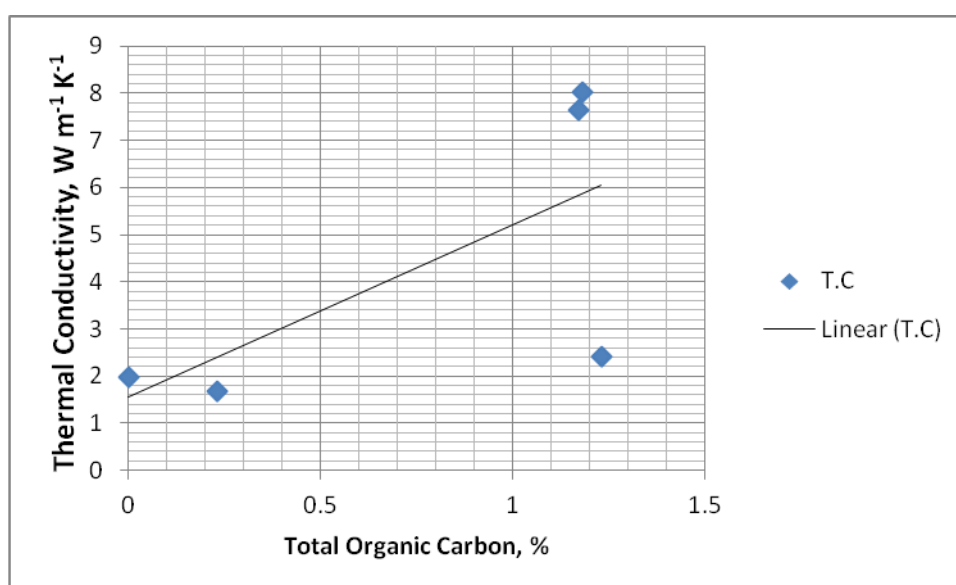


Figure 33: Thermal Conductivity vs. T.O.C

Based on the graphs, thermal conductivity is increasing with the accumulating amount of organic carbon. Organic carbon content within sandstone affected the

thermal conductivity coefficients, depending the types and amount of organic carbon accumulated within it.

4.10.3 Thermal Conductivity vs Porosity

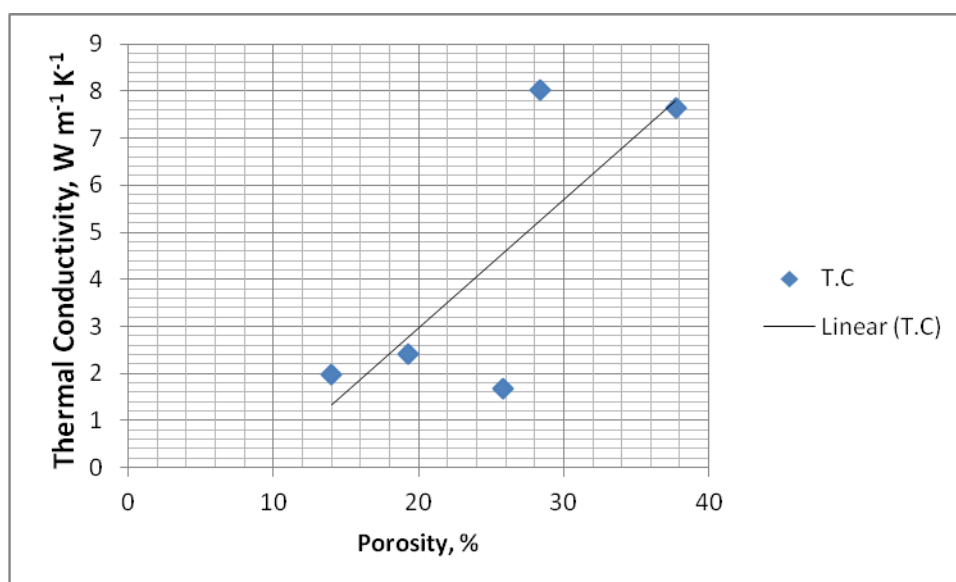


Figure 34: Thermal Conductivity vs. Porosity

One of the most important factors in determined thermal conductivity coefficient is porosity. Porosity means the measure of the void spaces within the sandstone. Initial investigation by previous literature review reveals that thermal conductivity increases with increase in effective stress of the rock (decrease in porosity). But in this experiment, this experiment displays the opposite side of it. By looking at the graph, thermal conductivity is directly proportional to porosity. There are numbers of factor that affected the relationship between thermal conductivity and porosity, which is possibly against the initial statement (literature review). Among them are;

- Mineralogy
 - Sandstone composed of mainly quartz. But there are different kinds of other minerals existed in it (as shown in the XRF results). For example, iron oxide, feldspar, muscovite and others. Each of these minerals displays different thermal conductivity, which indirectly affected the 'overall' thermal conductivity coefficient during

experiments. The heat flow within the sandstone samples have been affected by the heat conductivity found in different types of minerals.

- Grain contact
 - Thermal conductivity also affected by the grain contact. If the grain contact is high (very close to each other), heat loss during transfer between grain will be very small. Thus, heat flow could remain high. But, if the grain contact is low, there are void spaces in between the grains and it could be filled with air or fluid. These gas or water has their own conductivity. During heat transfer between the grain, heat will pass through the void spaces, resulting in loss of heat as well as affected by the gas or fluid conductivity. In usual case, with low grain contact, heat loss will be high, thus thermal conductivity is low.
- Special Particle Distribution
 - Special particle distribution refers to the characteristic of the fabric inside the rocks. By referring to the thin section, each samples display different types of fabric's characteristic. The grain size, particle arrangement, matrix and others. For example, in terms of grain size. By referring the thin section, outcrop 1 have relatively medium sized grain and high grain contact, resulting in higher thermal conductivity. But in outcrop 3, the grain size is small and grain contact is low. The void space (matrix) could be filled with air or fluid. Thus, with this condition, usually thermal conductivity is low because heat transfer between grains is low, but it could be high because is the heat transfer is affected be the heat conductivity that comes from the air or fluid filled-spaced.

CHAPTER 5: CONCLUSIONS AND RECOMMENDATIONS

The mineralogy and microscopy of some sedimentary rocks in Sarawak produce variety types of results, depending on the type of formation being studied. In the case, Nyalau Formation is the subject. Three outcrops from Nyalau formation (OC1, OC2 and OC3) have been selected to conduct research onto it, and produce results based upon the mineralogy and microscopy features. Most of the experiments that has been done have achieved the objective of this research. To conclude the research works;

5.1 CONCLUSION

Mineralogy and microscopy of the sedimentary rocks in Sarawak are different from each other compare, in terms of the three chosen outcrops location in Nyalau Formation. But majority of the common features of all the outcrops in Nyalau Formation are nearly identical as stated in previous literature reviews. To conclude the research work;

- For Thermal Conductivity, all outcrops have the same average of thermal conductivity value ($1 \text{ W m}^{-1} \text{ K}^{-1} - 10 \text{ W m}^{-1} \text{ K}^{-1}$) Thermal conductivity for sandstone is relatively low.
- For Fourier Transform Infrared Radiation, all outcrops contain aromatic functional group, such as Aryl C=C and Aryl-H, as well as other functional group such as CH=CH, C=N=N, O-H and others.
- For Ultraviolet, each outcrops produce nearly the same E4/E6 ratio (1.17 – 1.23). It means all outcrops nearly have the same degree of condensation of aromatic network of humic structures.
- For X-Ray Diffraction, most of the minerals exist in each outcrops contain quartz, as well as some feldspathic sandstone such as dolomite, pyrite, siderite, and hematite. Clay mineral also existed such as muscovite.
- For Ethylene Glycol Monoethyl Ether, the specific surface area (SSA) will help to determine the surface area size that will influence the reaction

characteristics and rate on the outcrops such as water retention, chemical and biological process. All outcrops have nearly the same average specific surface area (SSA), relatively between 21 m²/g - 33 m²/g, except for outcrop 2 which have the smallest SSA value, which is 9 m²/g.

- For Total Organic Compound, all outcrops have relatively very low TOC value, which is between 0% - 1.23%.
- For Hg Porosimeter, the porosity and permeability value vary with each outcrop. Outcrop 1 has the lowest porosity and permeability concentration while outcrop 3 has the highest porosity and permeability concentration. Outcrop 2 porosity and permeability concentration is in between of outcrop 1 and outcrop 3.
- For Scanning Electron Microscope, majority of the outcrops contain quartz, feldspar minerals, and few clay minerals such as muscovite which are commonly found within sandstone. But each grain shape and particle distribution is varying as discussed in Results and Discussions.
- For Thin Section, quartz grains are mostly observed as well as the possible existence of iron oxide mineral and coarse feldspar. The grain size and matrix is also differs among each outcrop as discussed in Result and Discussions.

5.2 RECOMMENDATION

The results from this research work can later be improved and expanded to better strengthen the findings and further justify the objectives that have been achieved.

- Conduct more literature review studies onto mineralogy and microscopy of sedimentary rocks as many of the scopes was already covered by some author such as E.S Hutchinson, Wan Abdullah Hasiah, Liehti & Haile, E.Padmanabhan, Shushan & Hadi and many more.
- Samples of sandstone need to be conducted experiments immediately as soon as being extracted from its outcrops. This is to retain the original composition as to not being exposed to different environments (temperature, pressure). The original composition could have produced more desired results.

- Samples need to be kept in cold, dried environments as the period of conducting experiments could expand from weeks to months. This is to retain the original composition within a long period of time.
- Reduce human and machine error. Most of the results obtain from samples are through human and machines works. If possible, conduct experiment with minimal error.
- Specific equipments and new experimental design should be used to better provide the best results for each sample.

CHAPTER 6: REFERENCES

- Teoh Ying Jia, USM; Characteristic of Sedimentary Facies and Reservoir Properties of Some Tertiary Sandstones in Sabah and Sarawak, East Malaysia, 2007C
- Zainol Affendi Abu Bakar, Mazlan Madon and Abdul Jalil Muhamad (PETRONAS Research and Technology Division: Deep-marine sedimentary facies in the Belaga Formation (Cretaceous-Eocene), Sarawak: Observations from new outcrops in Nyalau Formation mineralogical properties of some pyroclastic and sedimentary rocks- Ganesh Dhakal, 2006
- Adams, C.G. & Haak, R.; The stratigraphical succession in the Batu Gading area, middle Baram, north Sarawak, 1962
- Haile, N.S.; The geology and mineral resources of the Suai- Baram area, north Sarawak, 1962
- Liechti, P., Roe, RW. & Haile, N.S.; The geology of Sarawak, Brunei and the western part of North Borneo. *Geological Survey Department, British Territories in Borneo*, 1960
- Tan, D.N.K. & Hon, V.; *Geological field-guidebook. West Sarawak, Malaysia*, Geological Survey of Malaysia, Kuching, 1984
- Bruggen, Gerrit Ter.; De Eocene Fyllietformatie in Centraal-Borneo. Dissertation, University of Delft. [English translation by Haile, N.S] The Eocene Phyllite Formation in Central Borneo, 1995
- Teoh Ying Jia & Abdul Hadi Abdul Rahman; Comparative Analysis if facies and Reservoir Characteristic of Miri Formation (Miri) and Nyalau Formation (Bintulu), Sarawak, 2007

- J.P Andriesse; Characteristic and Formation of so-called Red-Yellow Podzolic Soils in the Humid Tropics (Sarawak, Malaysia), 1997
- Abdullah Wan Hasiah; Oil-generating potential of Tertiary coals and other organic-rich sediments of the Nyalau Formation, onshore Sarawak, 1999
- Masnan M.S, E. Padmanabhan, Mokhtar, M.A, Rajamohan G., and Prasanna V.; Thermal Conductivity values of Some Sandstone and Shale for the Belait Formation, GSm Newsletter, 2010
- C.Clausner & E.Huenges; Thermal Conductivity of Rocks and Minerals, 1995
- E.S Hutchinson; Geology of North West Borneo, 1987
- E. Padmanabhan; Impact of Spatial Variability in Microfabrics on Heat Transfer Characteristics of some Sedimentary Rocks, 2007
- P. Crews, J. Rodriguez & M. Jaspars; “Organic Structure Analysis”, 1998
- Joann E. Welton; “SEM Petrology Atlas”, The American Association of Petroleum Geologists, Tulsa, Oklahoma 74101, U.S.A., 2003

APPENDICES

Appendix 1: FYP 1 Gantt Chart

No.	Activities	Week													
		1	2	3	4	5	6	7	8	9	10	11	12	13	14
1	Topic Selection / Proposal							Mid-Semester Break							
2	Preliminary literature review on previous research papers/journals														
3	Laboratory experiment & observation														
4	Submission of proposal defence report														
5	Proposal Defence														
6	Plan Field trip to Sarawak (plan outcrops: Nyalau Formation)														

7	Analysis on research finding/data acquired & discussion														
8	Submission of Interim Draft Report														
9	Submission on Interim Report														

Appendix 2: FYP II Gantt Chart

No.	Activities	Week													
		1	2	3	4	5	6	7	8	9	10	11	12	13	14
1	Continue research work from FYP I							Mid-Semester Break							
	Thermal Conductivity														
	FTIR														
	UV-VIS														
	Thin Section														
	EGME														
	XRD														
	Hg Porosimeter														
	TOC														
	SEM														
2	Submission of Progress Report II														
3	Submission of Poster														
4	VIVA (Oral Presentation)														

5	Submission of Technical Paper														
6	Submission of Softbound														
7	Submission of Hardbound														

Appendix 3: Samples of Sandstones from Nyalau Formation

Unit 1 Outcrop 1

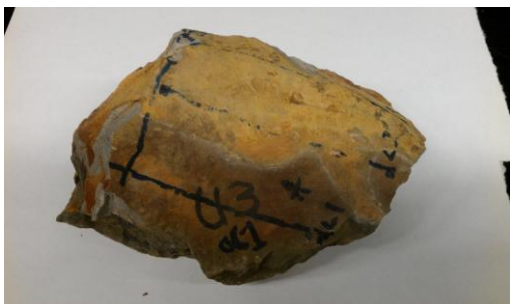


Face A



Face B

Unit 3 Outcrop 1



Face A



Face B

Unit 1 Outcrop 2



Face A



Face B

Unit 3 Outcrop 3



Face A



Face B

Unit 7 Outcrop 3



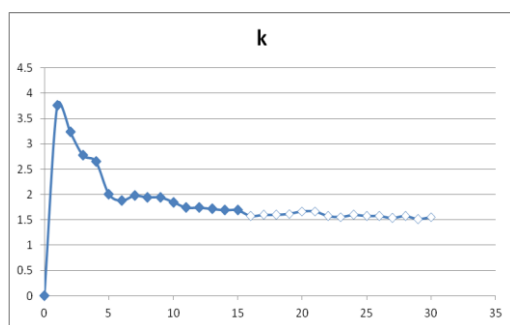
Face A



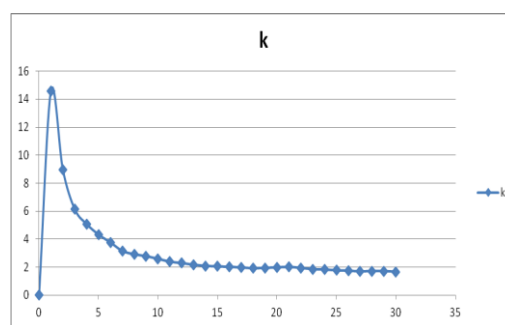
Face B

Appendix 4: Thermal Conductivity Results

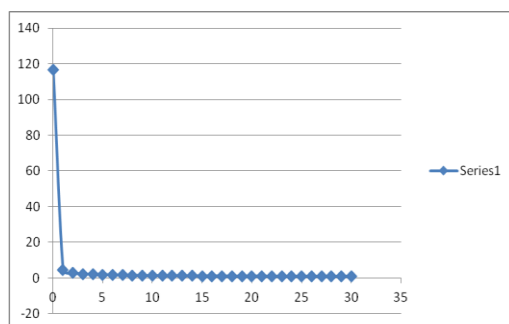
Unit 1 Outcrop 1 (U1 OC1)



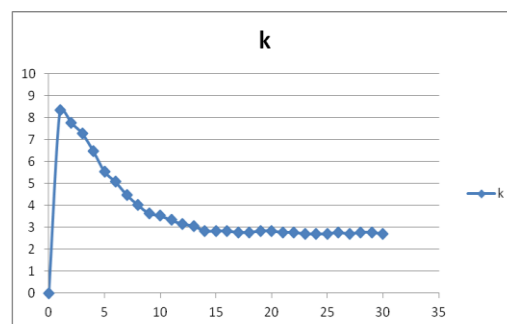
Line 1 Face A



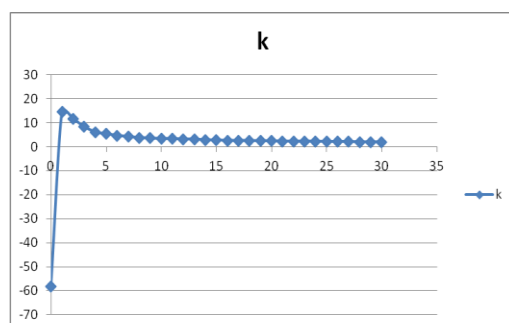
Line 1 Face B



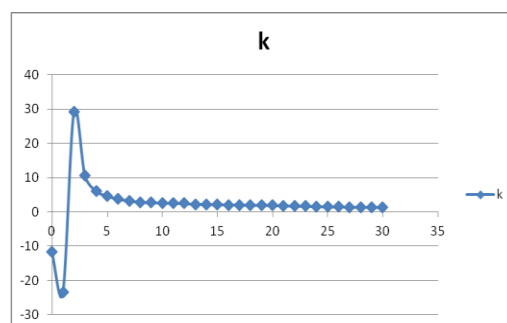
Line 2 Face A



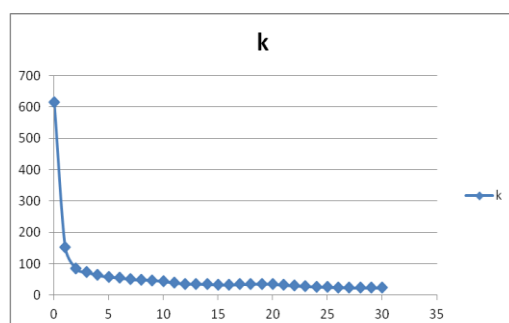
Line 2 Face B



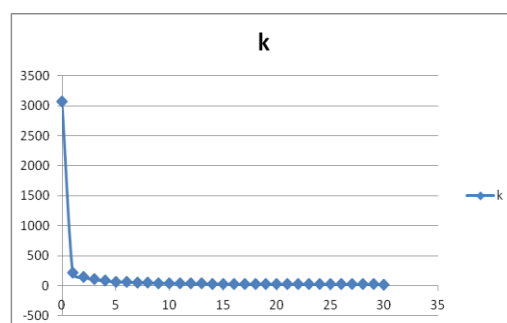
Line 3 Face A



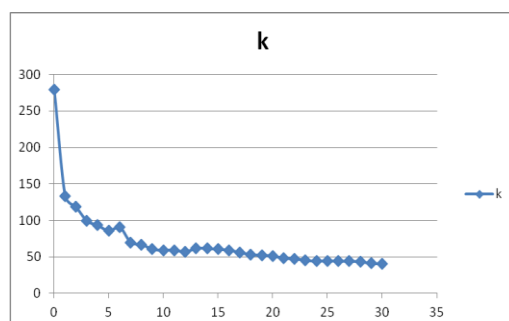
Line 3 Face B

Unit 3 Outcrop 1 (U3 OC1)

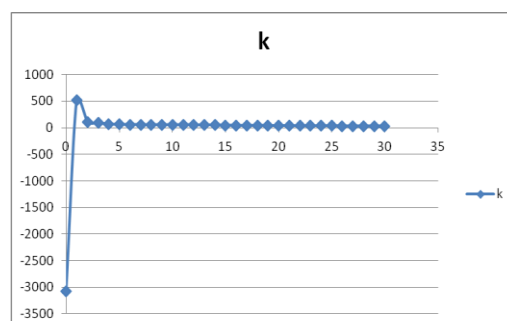
Line 1 Face A



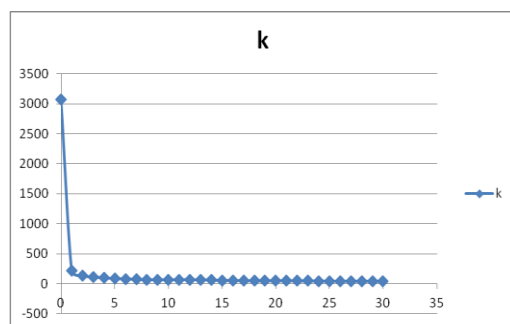
Line 1 Face B



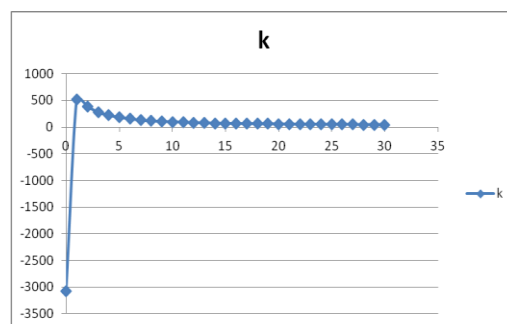
Line 2 Face A



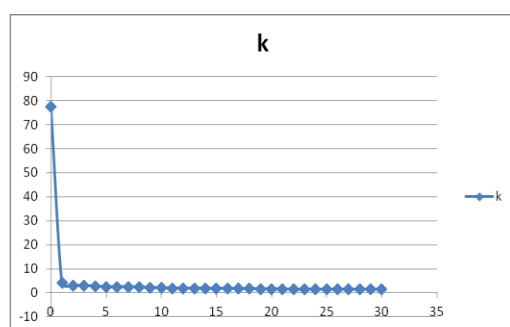
Line 2 Face B



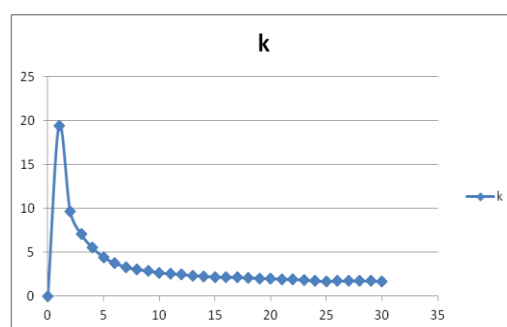
Line 3 Face A



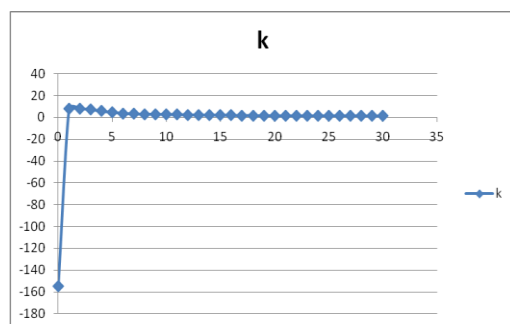
Line 3 Face B

Unit 1 Outcrop 2 (U1 OC2)

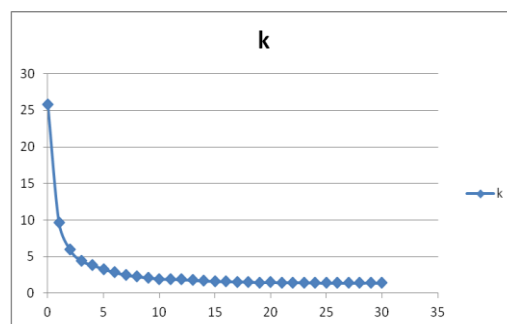
Line 1 Face A



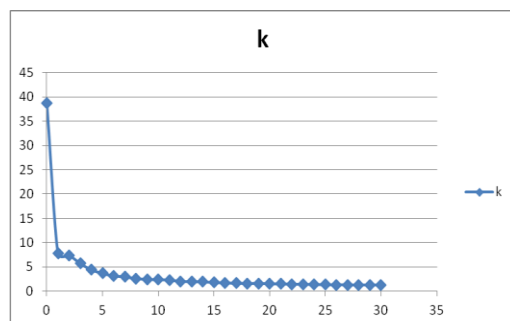
Line 1 Face B



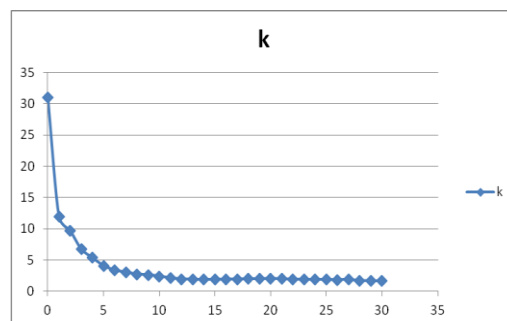
Line 2 Face A



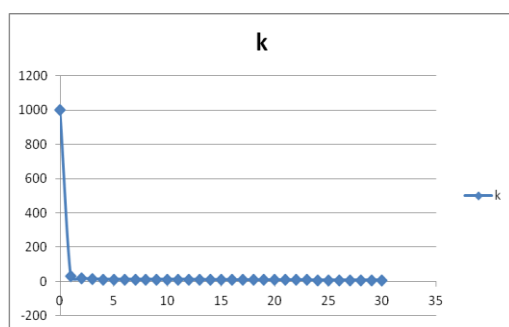
Line 2 Face B



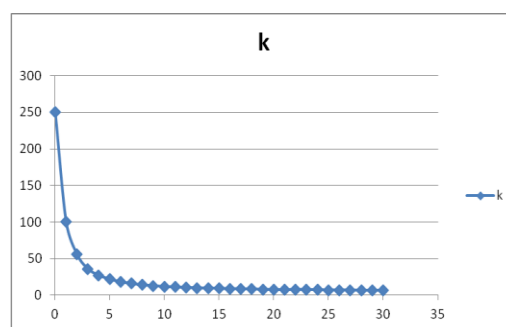
Line 3 Face A



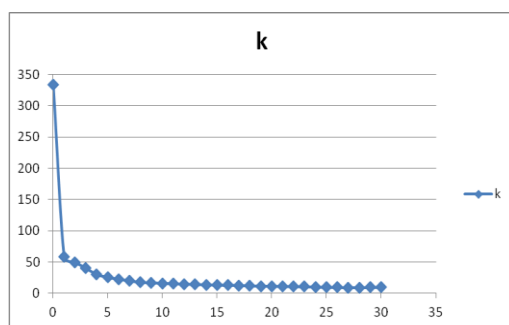
Line 3 Face B

Unit 3 Outcrop 3 (U3 OC3)

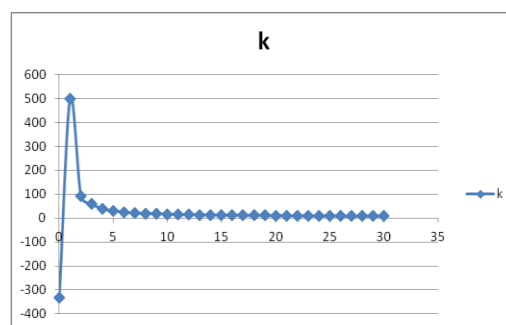
Line 1 Face A



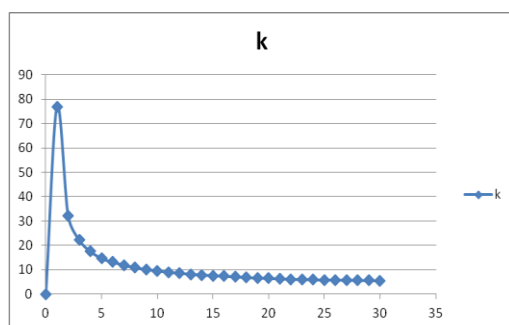
Line 1 Face B



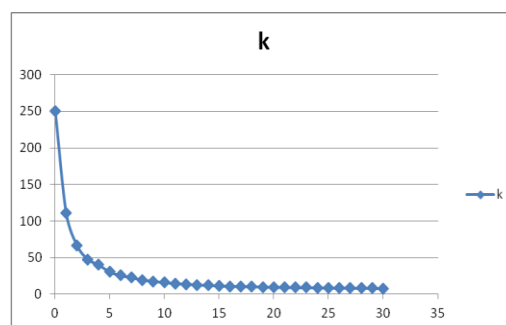
Line 2 Face A



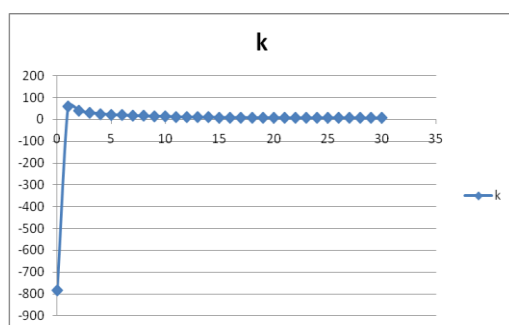
Line 2 Face B



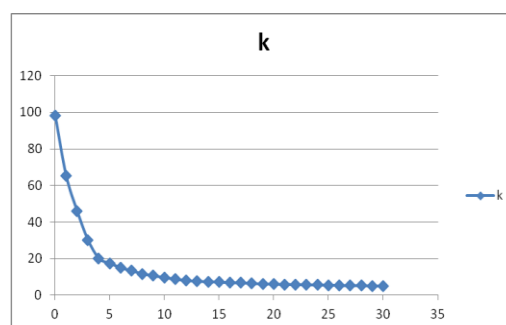
Line 3 Face A



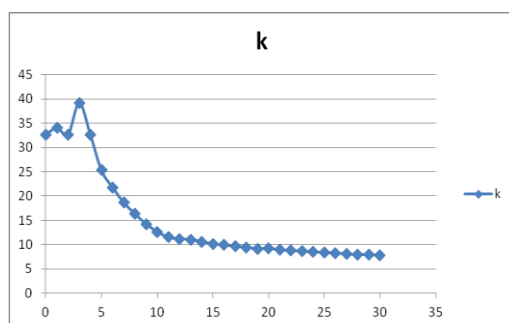
Line 3 Face B

Unit 7 Outcrop 3 (U7 OC3)

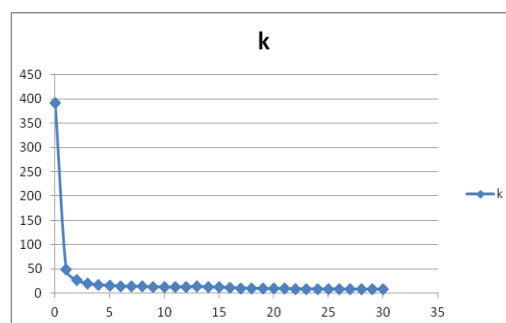
Line 1 Face A



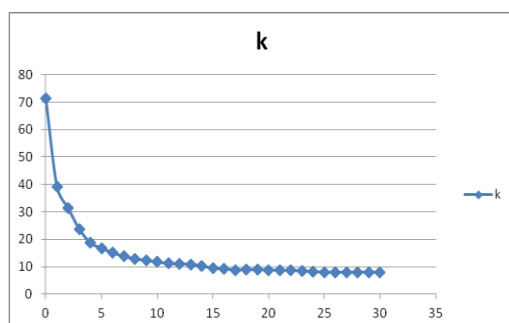
Line 1 Face B



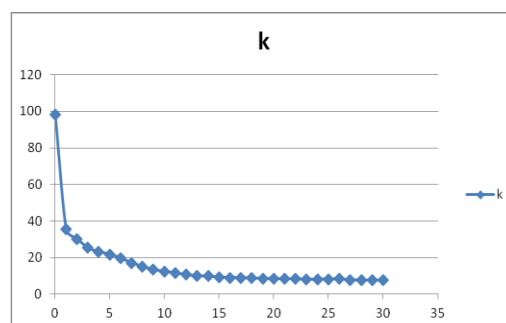
Line 2 Face A



Line 2 Face B



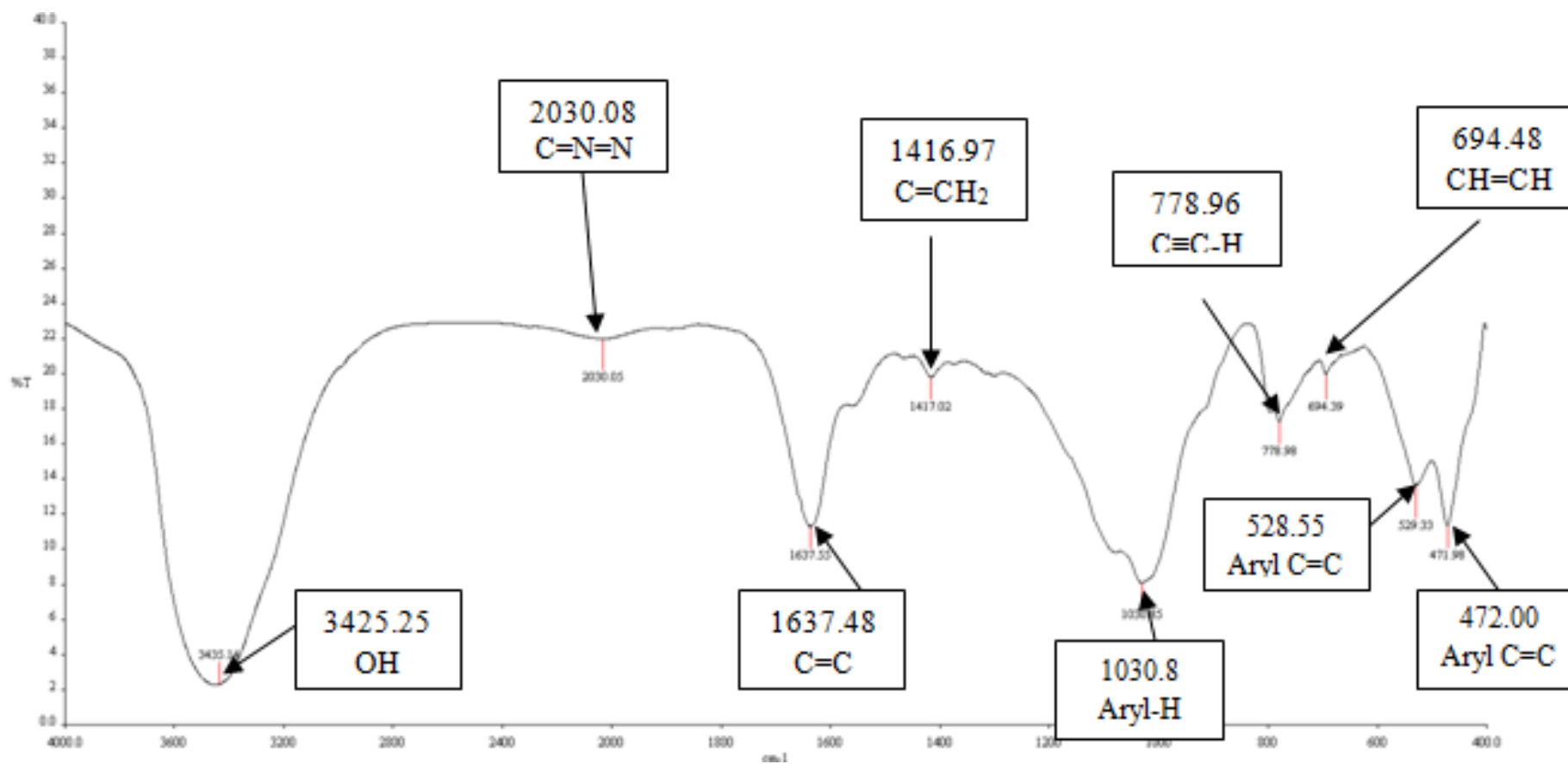
Line 3 Face A



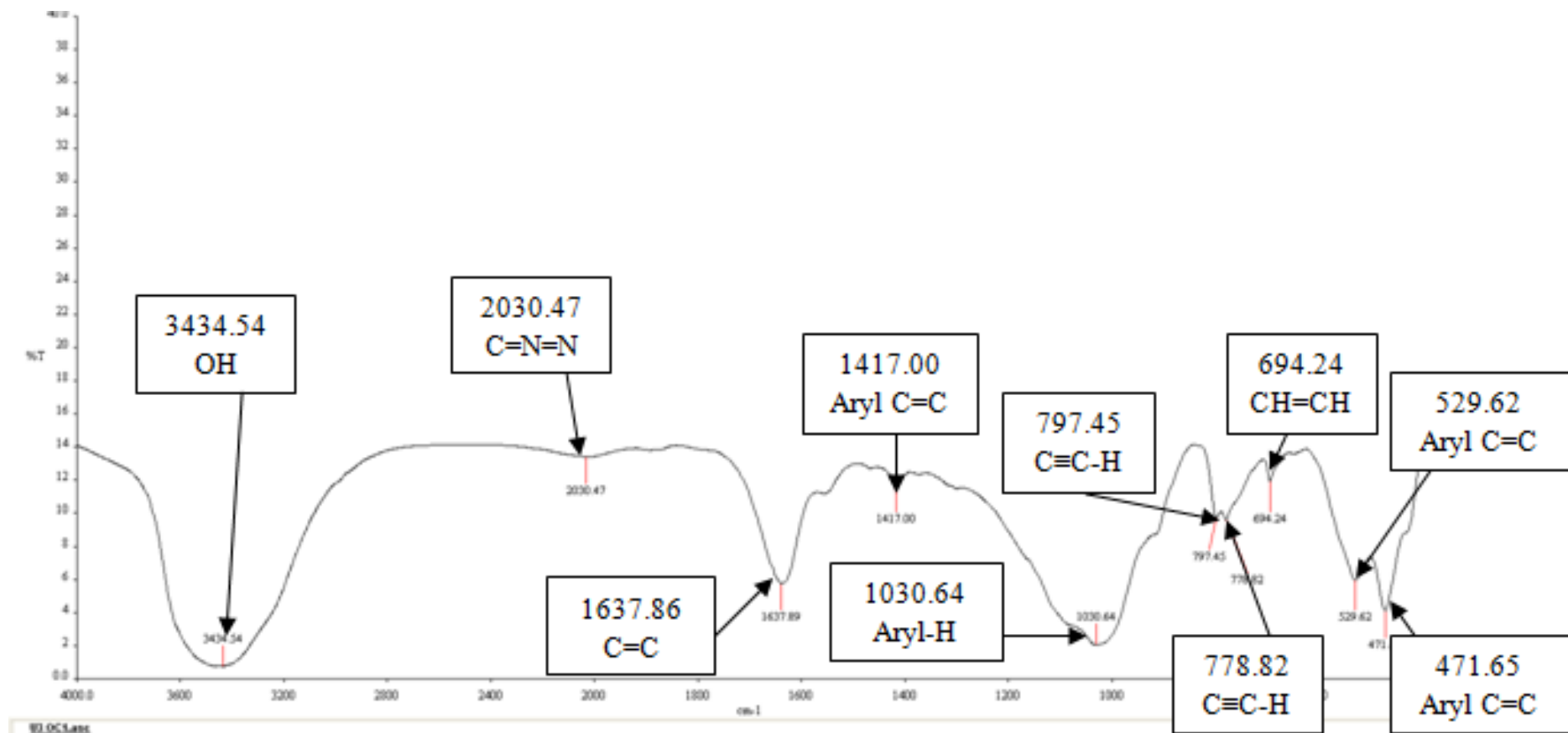
Line 3 Face B

Results on thermal conductivity are based upon the graphs [thermal conductivity (k) vs time, (minute)]

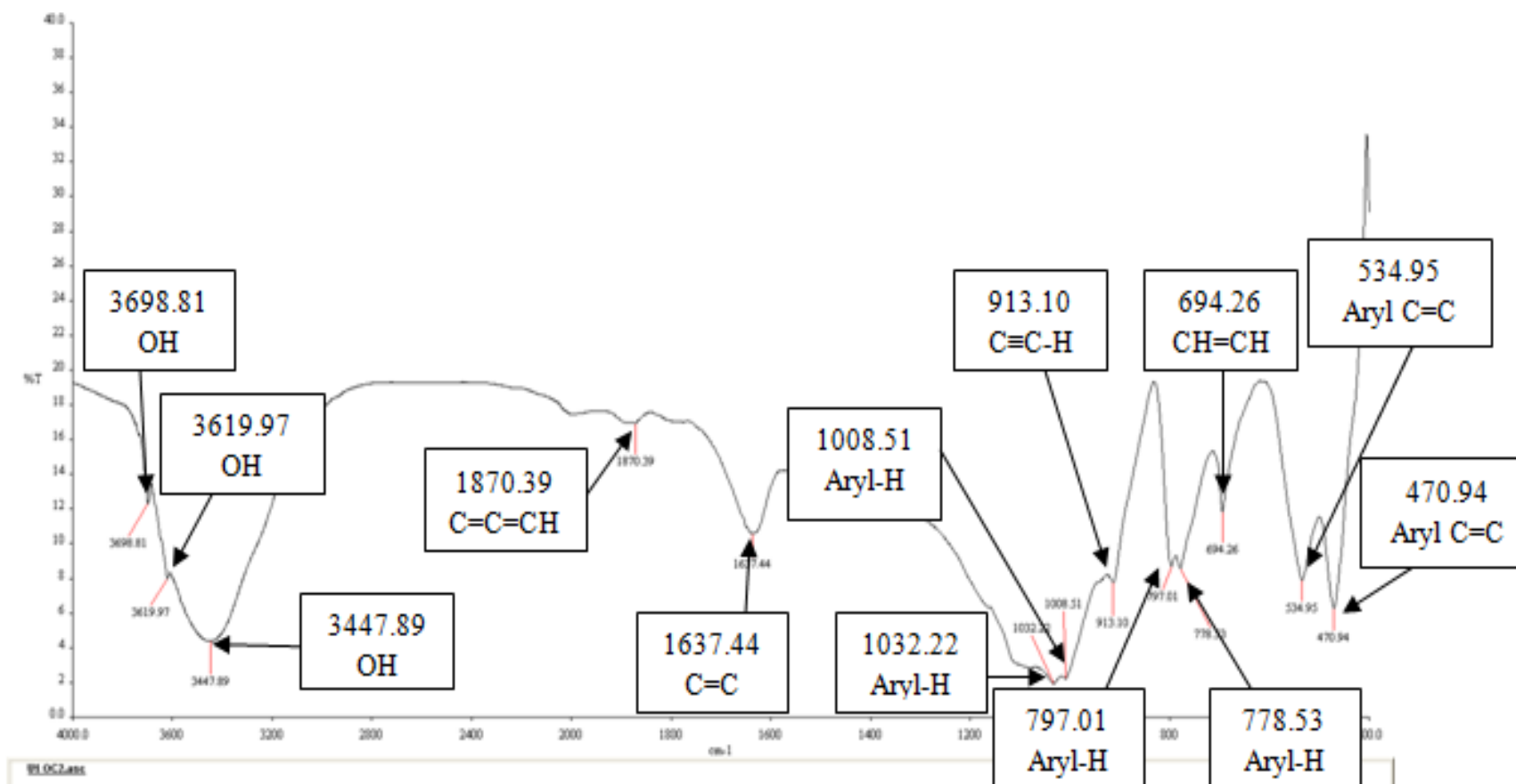
Appendix 5: Fourier Transform Infrared Radiation Results



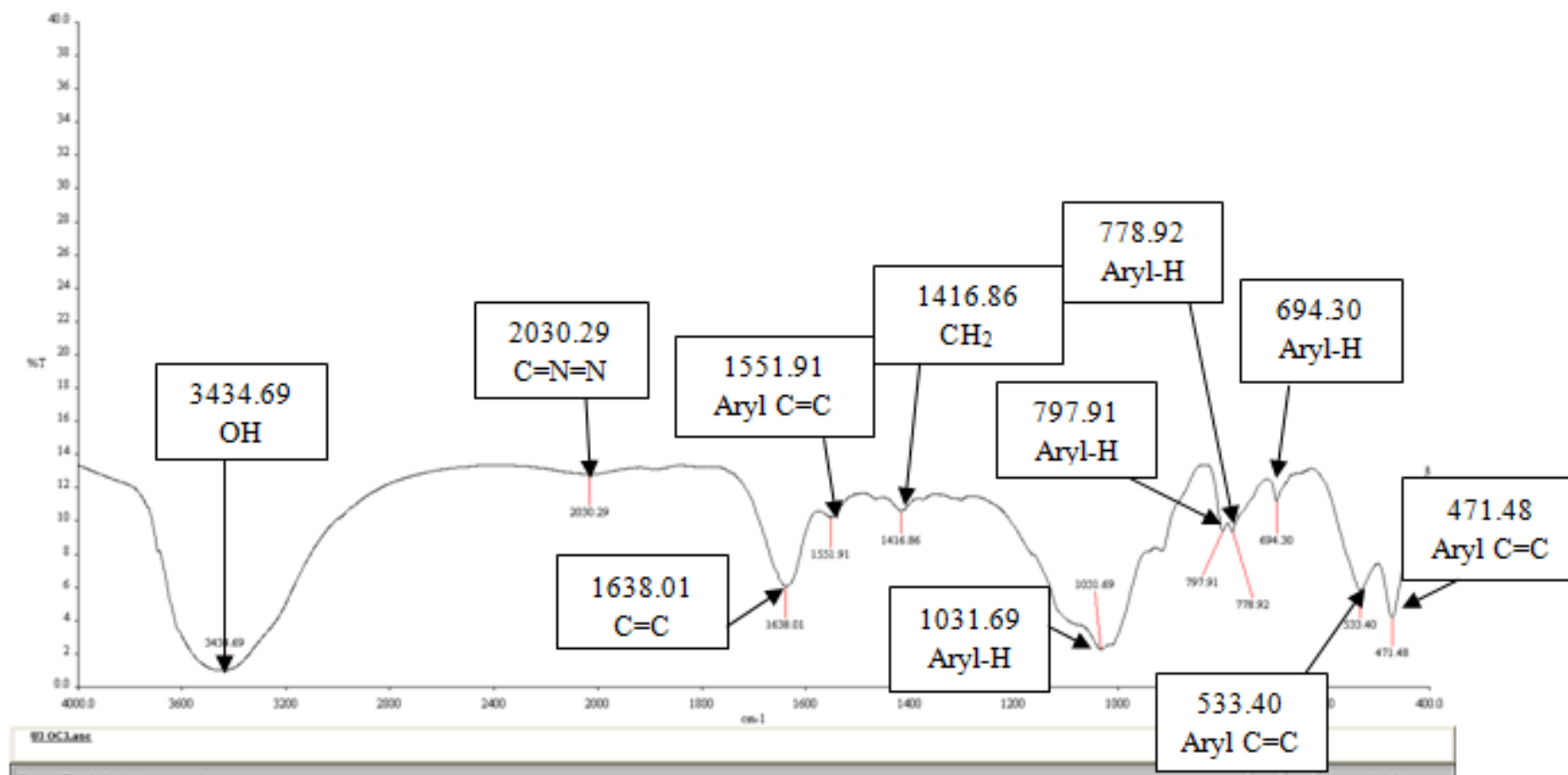
Unit 1 Outcrop 1



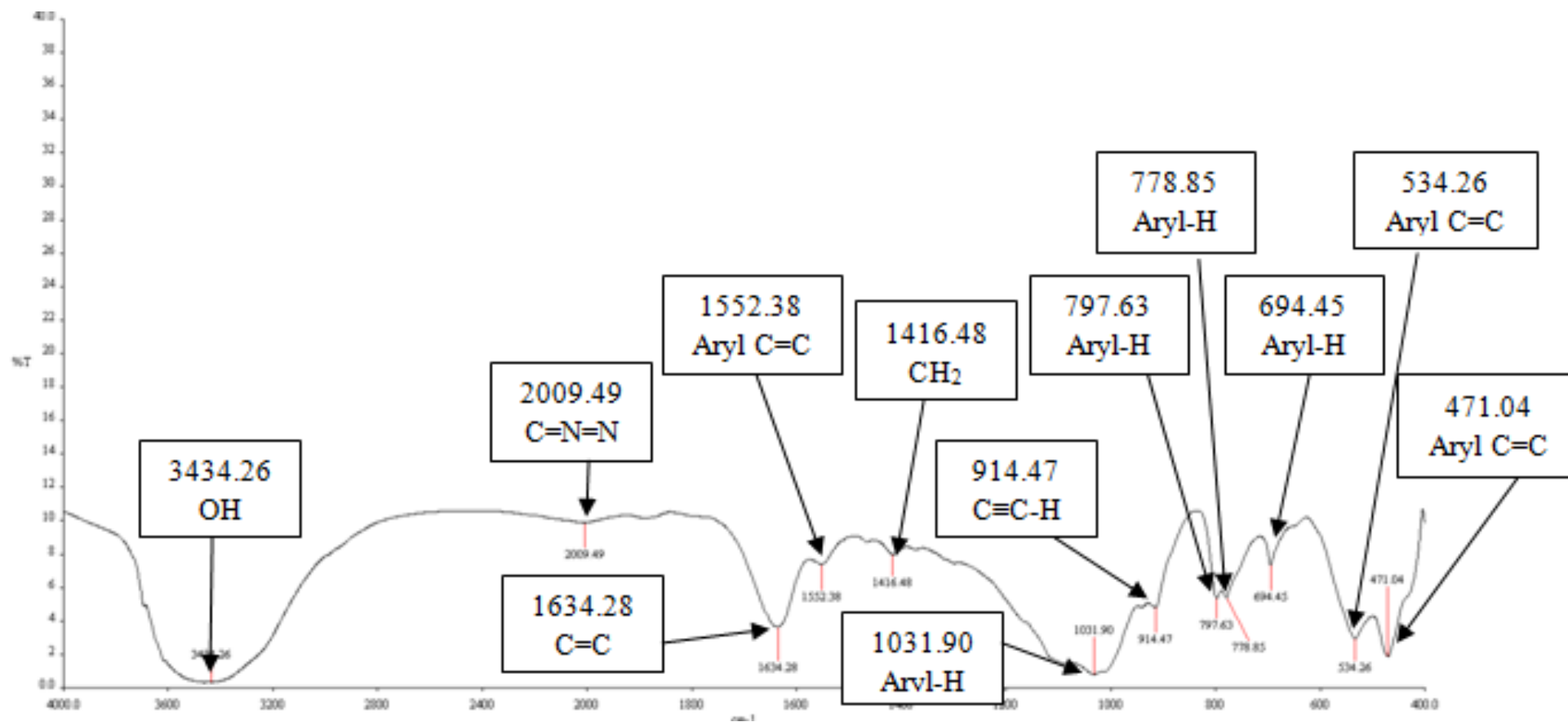
Unit 3 Outcrop 1



Unit 1 Outcrop 2



Unit 3 Outcrop 3

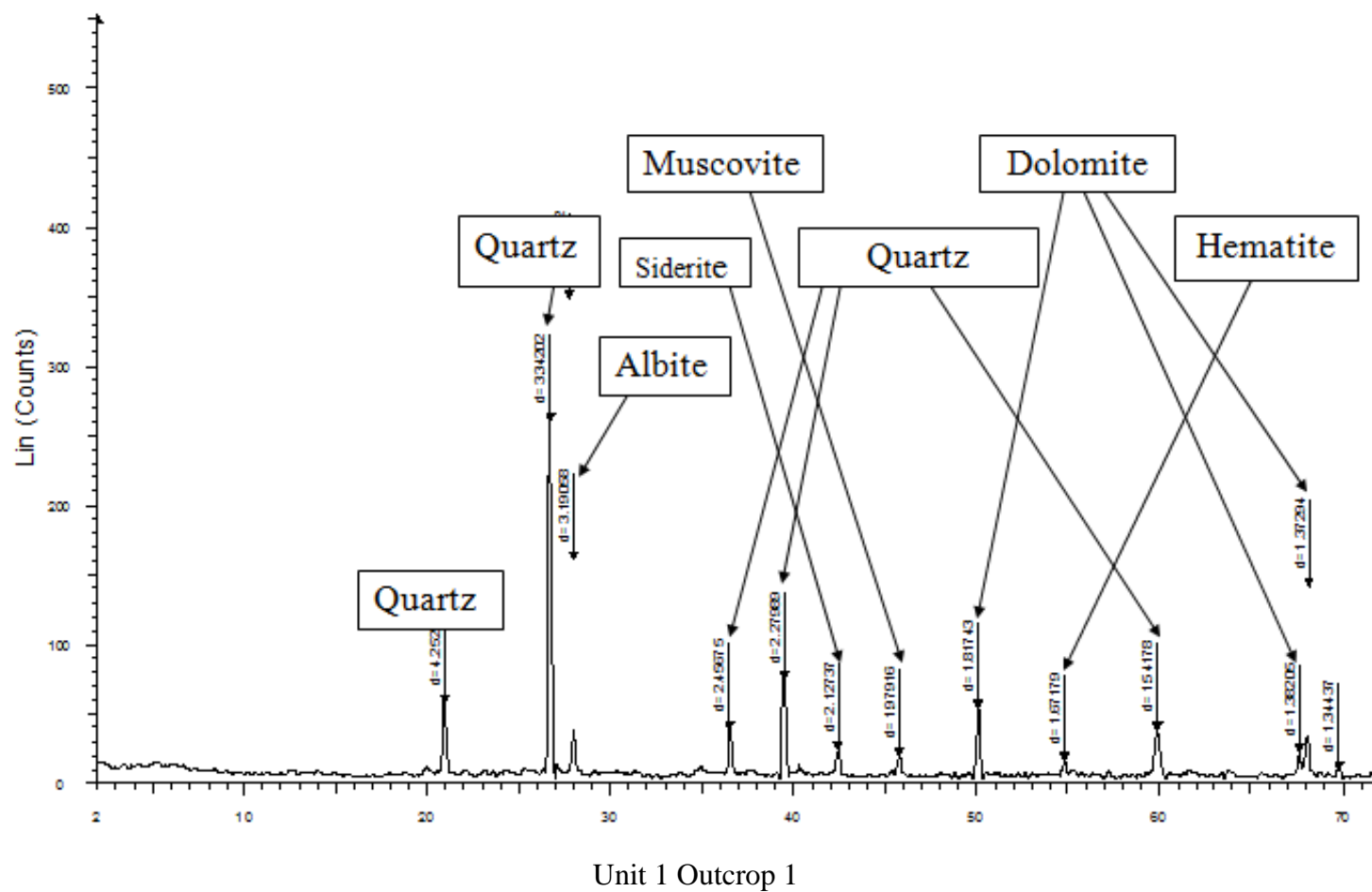


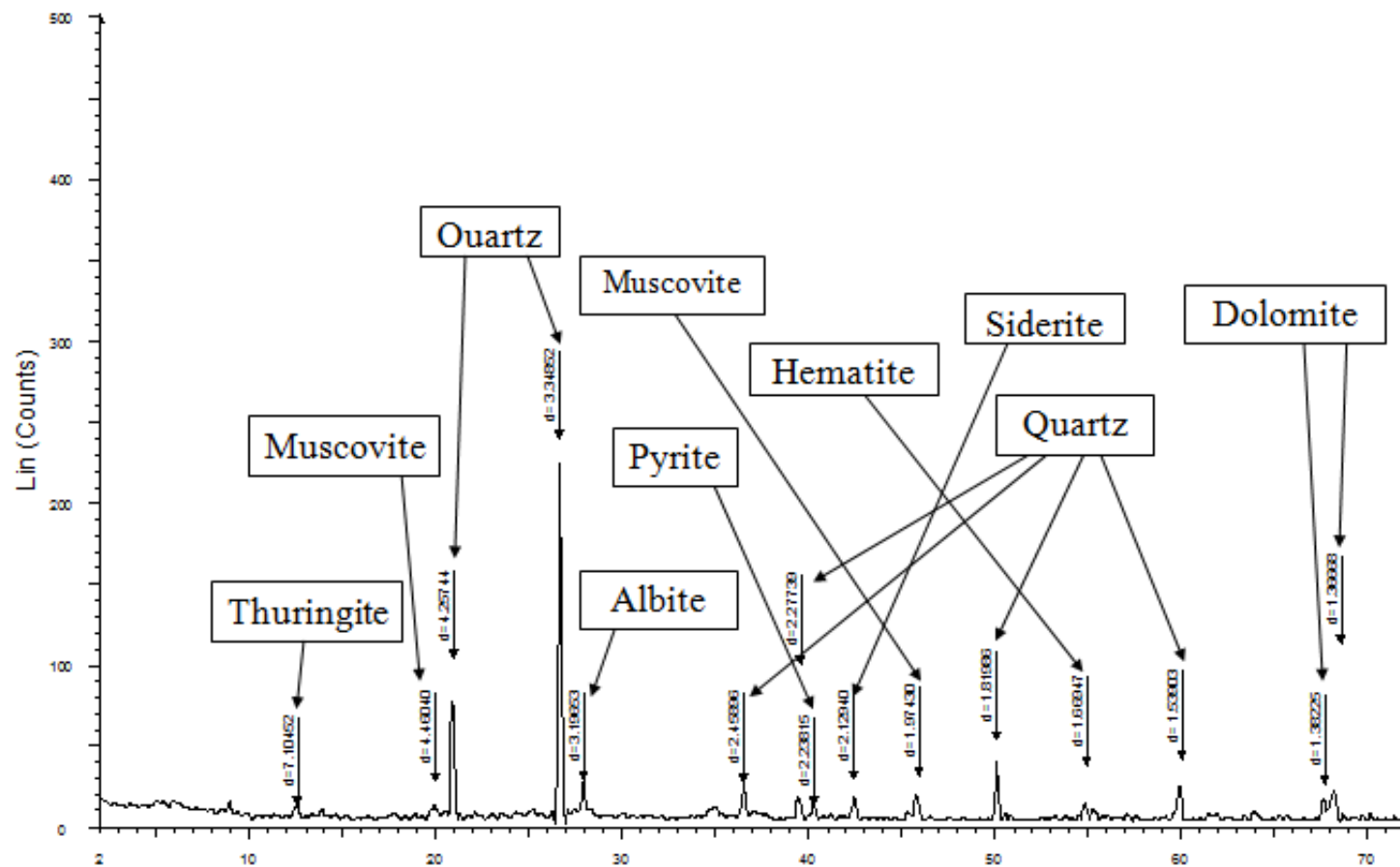
Unit 7 Outcrop 3

Appendix 6: Ultra Violet Table Results

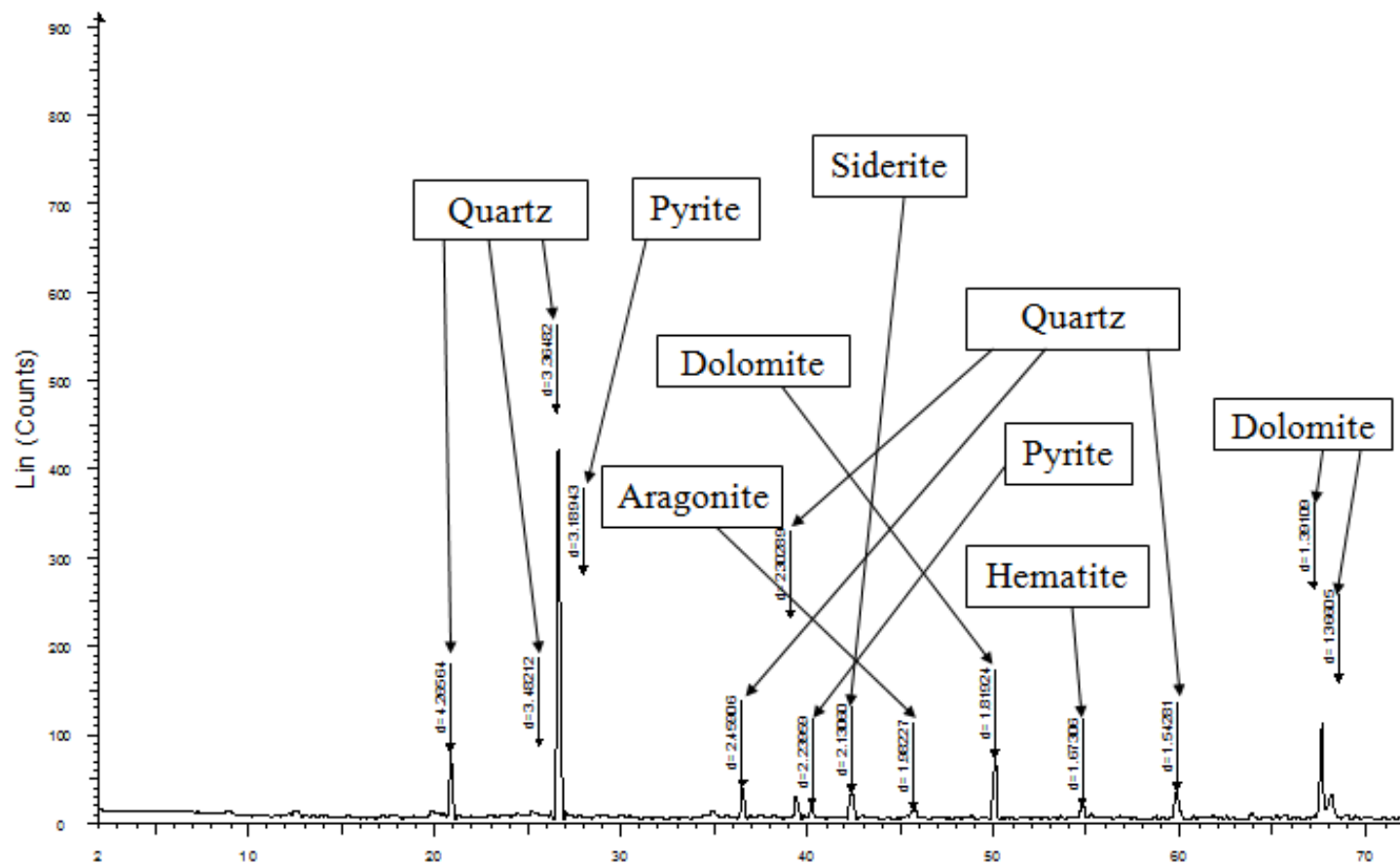
Wavelength nm.	U10C1	U30C1	U10C2	U3 OC3	U70C3
400	0.575	0.732	0.171	0.59	0.16
410	0.569	0.724	0.169	0.585	0.158
420	0.563	0.716	0.167	0.58	0.156
430	0.558	0.709	0.165	0.576	0.154
440	0.552	0.701	0.163	0.571	0.151
450	0.546	0.693	0.161	0.565	0.149
460	0.541	0.686	0.159	0.561	0.148
470	0.535	0.679	0.157	0.556	0.146
480	0.531	0.673	0.156	0.552	0.144
490	0.526	0.666	0.154	0.548	0.143
500	0.521	0.66	0.152	0.544	0.141
510	0.517	0.655	0.151	0.54	0.14
520	0.512	0.648	0.149	0.536	0.139
530	0.507	0.642	0.147	0.532	0.137
540	0.502	0.636	0.146	0.527	0.136
550	0.497	0.631	0.144	0.523	0.134
560	0.493	0.625	0.142	0.52	0.133
570	0.488	0.619	0.14	0.516	0.131
580	0.484	0.613	0.139	0.512	0.13
590	0.48	0.609	0.137	0.508	0.129
600	0.475	0.603	0.136	0.504	0.127
610	0.471	0.598	0.134	0.5	0.126
620	0.467	0.592	0.132	0.496	0.125
630	0.463	0.588	0.131	0.493	0.124
640	0.459	0.582	0.13	0.489	0.123
650	0.455	0.578	0.129	0.485	0.121
660	0.451	0.573	0.127	0.481	0.12
670	0.448	0.568	0.126	0.478	0.119
680	0.444	0.564	0.125	0.474	0.118
690	0.441	0.559	0.123	0.47	0.117
700	0.437	0.555	0.122	0.466	0.116
710	0.434	0.55	0.121	0.462	0.115
720	0.43	0.546	0.12	0.458	0.114
730	0.427	0.541	0.119	0.455	0.113
740	0.424	0.537	0.118	0.451	0.112
750	0.421	0.533	0.117	0.447	0.111
760	0.418	0.529	0.116	0.443	0.11
770	0.416	0.526	0.115	0.44	0.109
780	0.413	0.522	0.114	0.437	0.108
790	0.41	0.518	0.113	0.433	0.107
800	0.408	0.514	0.112	0.431	0.107

Appendix 7: X-Ray Diffraction Results

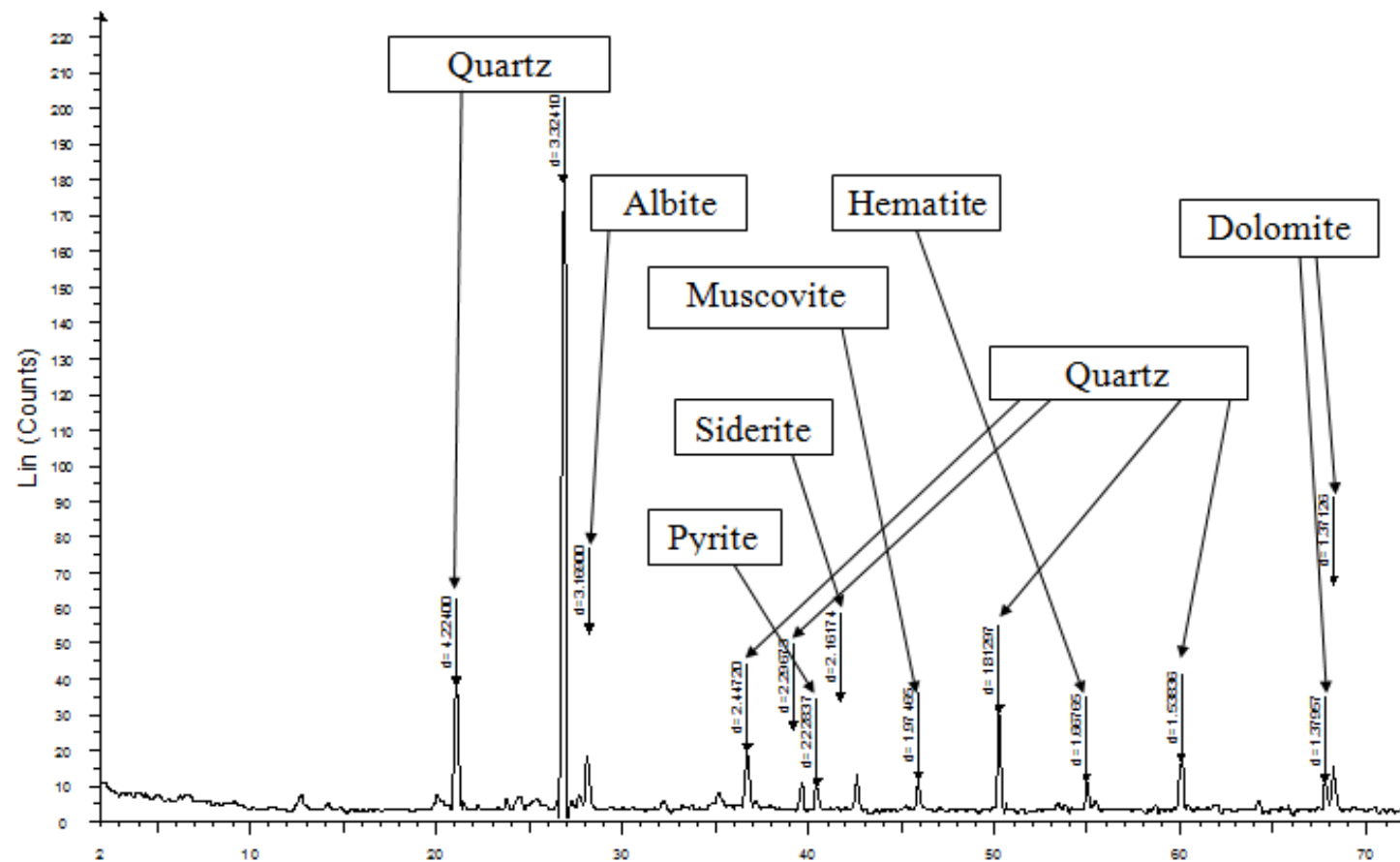




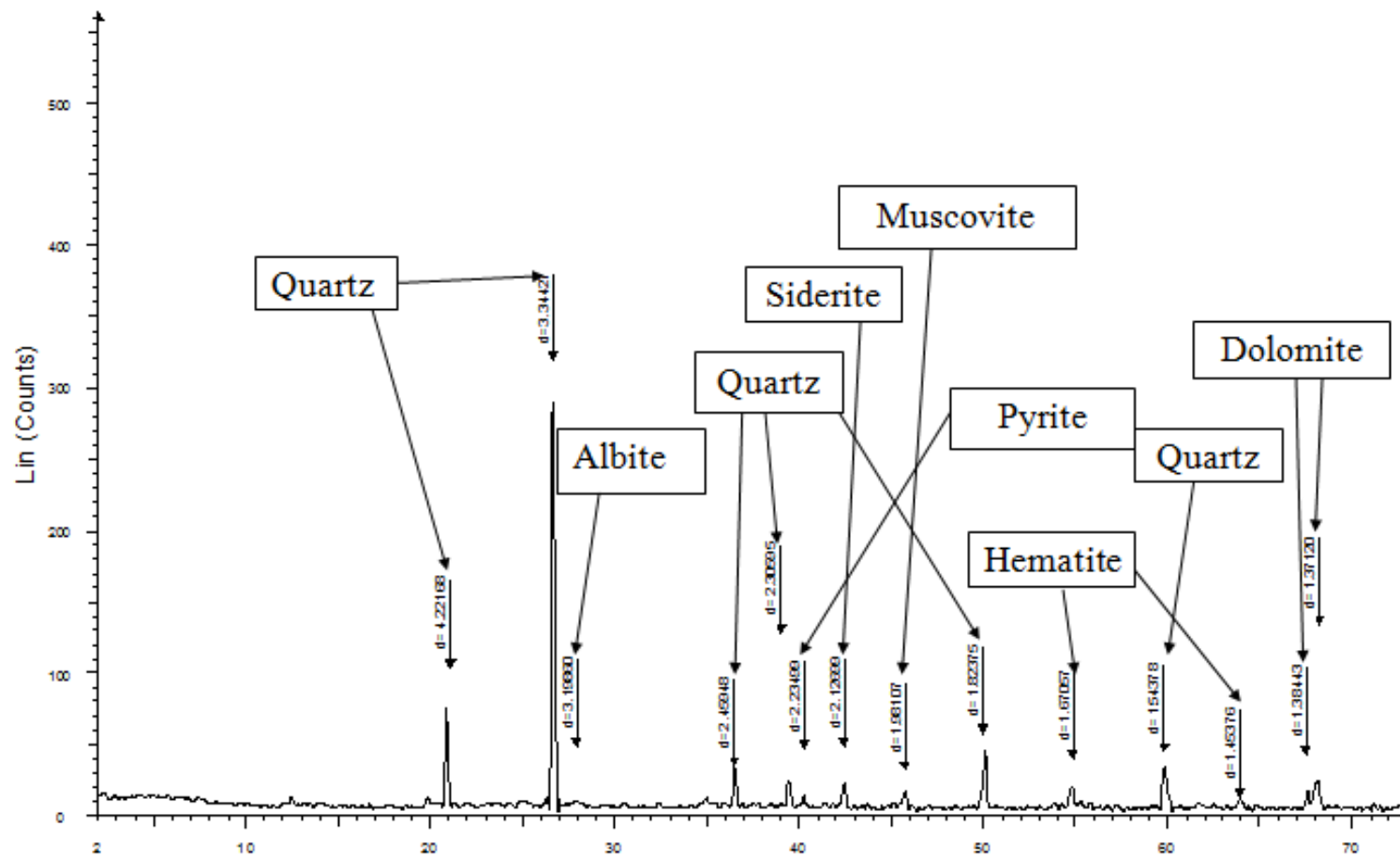
Unit 3 Outcrop 3



Unit 1 Outcrop 2



Unit 3 Outcrop 3



Unit 7 Outcrop 3

